AD_____

Award Number: W81XWH-06-1-0366

TITLE: Hunting for novel X-linked breast cancer suppressor genes in mouse and human

PRINCIPAL INVESTIGATOR: Yang Liu, Ph.D.

CONTRACTING ORGANIZATION: Ohio State University
Columbus, OH 43210

REPORT DATE: March 2007

TYPE OF REPORT: Final

PREPARED FOR: U.S. Army Medical Research and Materiel Command
Fort Detrick, Maryland 21702-5012

REPORT DOCUMENTATION PAGE

Form Approved
OMB No. 0704-0188

1. REPORT DATE *(DD-MM-YYYY)*	**2. REPORT TYPE**	**3. DATES COVERED** *(From - To)*
01/03/07	Final	15 Feb 2006 – 14 Feb 2007

4. TITLE AND SUBTITLE

Hunting for novel X-linked breast cancer suppressor genes in mouse and human

5a. CONTRACT NUMBER

5b. GRANT NUMBER
W81XWH-06-1-0366

5c. PROGRAM ELEMENT NUMBER

6. AUTHOR(S)
Yang Liu, Ph.D.

E-Mail: yang.liu@osumc.edu

5d. PROJECT NUMBER

5e. TASK NUMBER

5f. WORK UNIT NUMBER

7. PERFORMING ORGANIZATION NAME(S) AND ADDRESS(ES)

Ohio State University
Columbus, OH 43210

8. PERFORMING ORGANIZATION REPORT NUMBER

9. SPONSORING / MONITORING AGENCY NAME(S) AND ADDRESS(ES)
U.S. Army Medical Research and Materiel Command
Fort Detrick, Maryland 21702-5012

10. SPONSOR/MONITOR'S ACRONYM(S)

11. SPONSOR/MONITOR'S REPORT NUMBER(S)

12. DISTRIBUTION / AVAILABILITY STATEMENT
Approved for Public Release; Distribution Unlimited

13. SUPPLEMENTARY NOTES

14. ABSTRACT: A priori, X-linked tumor suppressor genes would be of great interest as one allele of these genes might be silenced due to X-chromosome inactivation. The X-linked Foxp3 is a member of the forkhead/winged helix transcription factor family. Germ-line mutations cause lethal autoimmune diseases in males. Serendipitously, we observed that Foxp3sf/+ heterozygous mice developed cancer at a high rate. The majority of the cancers were mammary carcinomas in which the wild-type Foxp3 allele was inactivated and ErbB2 was over-expressed. Foxp3 bound and repressed the ErbB2 promoter. Deletion, functionally significant somatic mutations and down-regulation of the FOXP3 gene were commonly found in human breast cancer samples and correlated significantly with HER-2 over-expression, regardless of the status of HER-2 amplification. In toto, the data demonstrate that FOXP3 is an X-linked breast cancer suppressor gene and an important regulator of the HER-2/ErbB2 oncogene.

15. SUBJECT TERMS
No subject terms provided

16. SECURITY CLASSIFICATION OF:			**17. LIMITATION OF ABSTRACT**	**18. NUMBER OF PAGES**	**19a. NAME OF RESPONSIBLE PERSON**
a. REPORT	**b. ABSTRACT**	**c. THIS PAGE**			USAMRMC
U	U	U	UU	69	**19b. TELEPHONE NUMBER** *(include area code)*

Standard Form 298 (Rev. 8-98)
Prescribed by ANSI Std. Z39.18

Table of Contents

Title: **Hunting for novel X-linked breast cancer suppressor genes in mouse and human**

Principal Investigator: Yang Liu, Ph.D.

Specific aims: 1. What are the *FoxP3* targets responsible for tumor suppressor activity? 2. What are the genetic mechanisms by which the *FOXP3* gene is inactivated in the majority of human breast cancer?

Study and results

We have completed the proposed work ahead of schedule because we have enlisted additional personnel than what was initially proposed. The major discoveries made are summarized below. These findings are presented in a manuscript which is currently being reviewed by Cell, the leading journal in Biology. We have also attached the manuscript as part of the report.

***1. FOXP3* is a repressor of *ErbB2* transcription**

HER-2/ErbB2 over-expression is critical for the growth of multiple breast cancer cell lines and confers a poor prognosis in breast cancer patients. To understand the mechanism by which disruption of *Foxp3* promotes tumorigenesis, we analyzed the expression of *ErbB2* in the normal and cancerous mammary tissues. We found that mammary cancer tissue from the $Foxp3^{sf/+}Otc^{spf/+}$ mice showed significant over-expression of ErbB2 as revealed by immunohistochemistry. Using real-time RT-PCR, 8-12-fold more *ErbB2* mRNA was found in the cancer cells than in normal epithelium There was also more *ErbB2* mRNA in the $Foxp3^{sf/+spf/+}$ epithelium than in that of the *WT* female mice, which indicates a potential gene dosage effect of *Foxp3* on the regulation of *ErbB2* expression in vivo. Transfection of the TSA cell line with *Foxp3* cDNA repressed *ErbB2* levels on the TSA cell line.

Increased activity of the *Her-2/ErbB2* promoter plays an important role in the over-expression of this oncogene in breast cancer. One potential mechanism by which *Foxp3* represses *Her-2/ErbB2* is to inhibit the promoter activity. Analysis of the 5' sequence of the *ErbB2* gene revealed multiple binding motifs for the forkhead domain. To test whether Foxp3 interacts with the *ErbB2* promoter, we used anti-V5 antibody to precipitate sonicated chromatin from the TSA cells transfected with the Foxp3-V5 cDNA and used real-time PCR to quantitate the amounts of the specific *ErbB2* promoter region precipitated by the anti-V5 antibodies in comparison to those that bound to mouse IgG control. The anti-V5 antibodies pulled down significantly higher amounts of *ErbB2* promoter DNA than the IgG control, with the highest signal around 1.6 kb 5' of the transcription starting site.

To test whether the binding correlated with the suppression by Foxp3, we produced luciferase reporter using the 1.8, 1.2 and 0.8 Kb upstream of the *ErbB2* TSS and tested the ability of Foxp3 to repress *ErbB2* promoter activity. In three separate cell lines, we observed that the region with the strongest ChIP signal was required for optimal repression by Foxp3. Furthermore, we deleted two *Foxp3*-binding sites conserved between mouse and human by site-directed mutagenesis and measured the effect on Foxp3-mediated repression. Deletion of either binding site substantially increased the

ErbB2 promoter activity in the presence of Foxp3 and thus alleviated Foxp3-mediated repression.

Since mutant B also showed a significant reduction in basal promoter activity, it is theoretically possible that loss of suppression by Foxp3 may be linked to the loss of another enhancer. As such, Foxp3 may only indirectly affect the *ErbB2* promoter. To rule out this possibility, we first used an electrophoretic mobility shift assay (EMSA) to determine whether the forkhead DNA-binding motifs in region B bound to Foxp3. The nuclear extracts from the *Foxp3*-expressing cells specifically retarded migration of the WT but not mutant ^{32}P-labeled probes compared with control cells. Since our Foxp3 antibodies could not be used for the super-shift assay, we performed oligonucleotide competition analysis. While mutant cold probes did not affect Foxp3 binding activities, WT cold probes significantly diminished them, establishing that the binding of these complexes is specific to forkhead DNA-binding motifs. Based on these data, we carried out site-directed mutagenesis to replace the 12 nucleotides (mut C) within the *ErbB2* promoter and compared the promoter activity and Foxp3-repression by luciferase assays. While the wild-type promoter was repressed by Foxp3, no repression by Foxp3 was observed when the mutant promoter was used. Moreover, in contrast to the deletional Mut B, the mutations had no impact on the basal activity of the *ErbB2* promoter. Taken together, our new data make a compelling case that Foxp3 represses the ErbB2 promoter via specific forkhead binding motifs.

***2. FOXP3* defects in human breast cancer**

We analyzed the levels and isoforms of the *FOXP3* transcripts in a panel of normal human mammary epithelial cells (HMEC), an immortalized but non-malignant cell line (MCF-10A), and 10 malignant breast cancer cell lines differing in ER/PR and HER-2 status. Similar levels of *FOXP3* transcripts were observed in two lines of HMEC and in the immortalized cell line MCF-10A. Each of the 10 tumor cell lines had a different degree of reduction in *FOXP3* mRNA levels in comparison to HMEC and MCF-10A. Among them, 2 were completely devoid of FOXP3 mRNA, while the others had a 1.5-20 fold reduction. We then used anchored primers spanning exons 1-12 to amplify the FOXP3 transcripts, and then we sequenced the PCR products. None of the tumor cell lines expressed full-length *FOXP3* transcripts. The HMEC expressed the same two isoforms as observed in the T cells, while MCF-10A expressed the exon 3-lacking isoform which was somewhat less functional than the full length FOXP3 in repressing proliferation of human T cells. The same isoform was also found in 4 tumor cell lines at much lower levels. In addition, 3 tumor cell lines expressed an isoform lacking both exons 3 and 4. The alternative splicing resulted in a frame-shift beginning at codon 70 and an early termination at codon 172. Furthermore, 2 tumor cell lines expressed a FOXP3 isoform lacking exons 3 and/or 8. Exon 8 encodes the leucine-zipper domain that is frequently mutated in IPEX patients. Thus, FOXP3 is abnormal in breast cancer cell lines. Consistent with a role for *FOXP3* in repressing *HER-2* expression, the majority of the breast cancer cell lines had higher levels of HER-2 in comparison to normal HMEC. However, additional changes are also likely required for *HER-2* over-expression, as three cell lines did not over express *HER-2* even though the *FOXP3* transcripts were greatly reduced.

We took three approaches to determine whether the findings in the mutant mice and human breast cancer cell lines are relevant to the pathogenesis of human breast cancer. First, we used immunohistochemistry to determine expression of FOXP3 in normal vs. cancerous tissue. While more than 80% of the normal breast samples expressed FOXP3 in the nuclei of the epithelial cells, less than 20% of the cancerous tissue showed nuclear staining. The difference between normal and cancerous tissue was highly significant ($P=6.0x10^{-16}$). Reduced expression of FOXP3 was observed among ER^+ ($P=1.0x10^{-7}$) and ER^- ($P=8.2x10^{-18}$) cancer samples, although more severe reduction was observed in the ER^- than in the ER^+ tumor group (P=0.002). RT-PCR revealed that the *FOXP3* transcripts in the primary human mammary epithelial cells (HMEC) contained two major forms that were found in human T cells.

Second, we used fluorescence in situ hybridization (FISH) to determine whether the *FOXP3* gene was deleted in the breast cancer samples. The minimal common region of deletion was identified using flanking p-telomeric and centromeric clones. Out of 223 informative samples, we observed 28 cases (12.6%) with deletions in any of the three loci. Interestingly, deletion of the *FOXP3* locus was found in all of the 28 cases. These data suggest that *FOXP3* is likely within the minimal region of deletion in the Xp11 region studied. Although all deletions were heterozygous, the FOXP3 protein was undetectable in 26/28 cases. Thus, it appears that for the majority of the breast cancer samples, LOH alone was sufficient to inactivate the locus, perhaps due to X-chromosomal inactivation. The two cases with both deletion and FOXP3 expression had X-polysomy with 3 and 4 X-chromosomes respectively.

Thirdly, we isolated DNA from matched normal and cancerous tissues (50 cases with formalin fixed samples and 15 cases of frozen samples) from patients with invasive ductal carcinoma and amplified all 11 coding exons and intron-exon boundary regions by PCR. Two independent PCR products were sequenced in order to confirm the mutations. Unless the bulk sequencing data were unambiguous, the PCR products were cloned and 5-10 independent clones from each reaction were sequenced. Among the formalin fixed samples, we only used the cases in which the normal tissue samples gave unambiguous sequencing data that matched the wild-type *FOXP3* sequence. When the cancerous tissues were compared with normal tissues from the same patient, 36% (18/50 formalin-fixed samples and 5/15 frozen samples) showed somatic mutations. Loss of wild-type allele was found in 6/23 cases (38%) of cancer samples with somatic *FOXP3* mutations. The other cases had heterozygous mutation. Eighteen mutations resulted in the replacement of amino acids in domains. Most are likely to be critical for FOXP3 function, as judged from the pattern of mutation in IPEX patients or in the conserved zinc finger domain that has so far not been implicated.

Although most samples had a single mutation of the *FOXP3* gene, we did observed two cases with multiple mutations. In the first sample, the two mutations occurred in consecutive codons, resulting in two nonconservative replacements of amino acid residues. Clonal analysis revealed that both mutations occurred in the same clone. In the second sample, three mutations occurred in intron 11. Since this case lacked a WT allele, it is likely that all of the mutations occurred in the same allele. The possibility of a mismatch in the cancer and normal samples was ruled out by comparing the normal and cancer samples for polymorphism of two unrelated genes. One was the *CD24* gene in chromosome 6 and the other was the X-linked *OTC* gene.

To directly test whether FOXP3 mutations affect the repressor activity for the *HER-2* gene, we chose two representative somatic *FOXP3* mutants isolated in the cancer cells and tested their repressor activity for the *HER-2* promoter. One mutation (338P>L) resided in the signature forkhead domain which is often mutated in the IPEX patient, while the other double mutation (*204C>R205E>K*) was from the zinc finger domain that has not been implicated in IPEX patients. Both mutations significantly reduced the repressor activity of FOXP3. The reduced repression of the *HER-2* promoter correlates with a significantly reduced inhibition of *HER-2* mRNA.

Four cases had mutations in introns that may potentially affect RNA splicing. We used laser-guided micro-dissection to isolate normal and cancerous epithelial cells from one case with a mutation in intron 6 (case 23). RNA was isolated and tested for the potential effect of the mutation on RNA splicing (using primers on exons 5 and 8) and total *FOXP3* transcript, as quantitated by real time PCR using primers spanning exons 10-12. Tissues from another patient with a mutation in exon 7 were used as control. Primers spanning exons 5 and 8 failed to detect *FOXP3* mRNA from the cancerous tissue of case No. 23. Furthermore, primers spanning exons 10-12 also failed to detect any *FOXP3* transcripts. Substantial levels were detected in the normal epithelial cells of the same patients as well as in normal and cancerous tissues from case No. 22. Since the wild-type allele had been lost in the cancer cells of case No. 23, it is likely that the mutation in intron 6 inactivated *FOXP3.* With an intron of 944 nucleotides, a mutation that prevented splicing of intron 6 would cause premature-termination codon-mediated RNA decay, which is operative in the *FOXP3* gene. These results demonstrate that the *FOXP3* locus is targeted in breast cancer by a number of different mechanisms, including deletion, somatic mutation and other unknown mechanisms of silencing. Since the samples used for mutational analysis are limited and do not completely overlap with those used for FISH, it is unclear whether these two mechanisms act in concert to inactivate the *FOXP3* locus.

***3. FOXP3* defects and HER-2 over-expression**

We have obtained five lines of evidence that support a critical role for *FOXP3* in the repression of the *HER-2* oncogene in human breast cancer. First, we silenced the *FOXP3* gene in primary HMEC using a lentiviral vector expressing *FOXP3* siRNA. The *FOXP3* siRNA reduced *FOXP3* expression by more than 100-fold while increasing *HER-2* mRNA by 7-fold. A corresponding increase in cell surface HER-2 was also observed. These results implicate *FOXP3* as a repressor of *HER-2* in human breast epithelial cells. Second, since a major mechanism for HER-2 up-regulation in breast cancer is gene amplification, an intriguing issue is whether *FOXP3* is capable of repressing HER-2 in cancer cells with an amplified HER-2 gene. We produced a Tet-off line of BT474, a breast cancer cell line known to have HER-2 gene amplification, and transiently transfected it with a *pBI-EGFP-FOXP3*- vector. After drug selection, the cells were cultured either in the presence or absence of doxycycline. While the cells cultured with doxycycline did not express FOXP3, removal of doxycycline resulted in induction of FOXP3 in a significant fraction of the cancer cells, which allowed us to compare HER-2 levels in the $FOXP3^+$ and $FOXP3^-$ cells in the same culture by flow cytometry. $FOXP3^-$

cells had about a 5-10-fold higher level of HER-2 protein on the cell surface in comparison to the $FOXP3^+$ cells. These results demonstrate that FOXP3 can suppress HER-2 expression even in cells with multiple copies of the HER-2 gene.
Thirdly, we compared the expression of FOXP3 with HER-2 expression in breast cancer tissues. Down-regulation of FOXP3 was strongly associated with the over-expression of HER-2, which supports a role for *FOXP3* inactivation in *HER-2* over-expression in breast cancer. Nevertheless, since many of the $FOXP3^-$ cells remained $HER\text{-}2^-$, it is likely that dis-regulation of *FOXP3* is insufficient for *HER-2* up-regulation. On the other hand, since only 3/82 $FOXP3^+$ cancer cells expressed high levels of HER-2, *FOXP3* inactivation is likely important for *HER-2* up-regulation under most circumstances.
Fourth, we divided breast cancer samples based on their *HER-2* gene copy numbers and compared the $FOXP3^+$ and $FOXP3^-$ cancer samples for the relative amounts of cell surface HER-2 expression. In each of the gene dose categories, $FOXP3^+$ samples had reduced HER-2 scores in comparison to the $FOXP3^-$ samples. These results strongly suggest a critical role for FOXP3 in repressing HER-2 expression even in the cases of the *HER-2* gene amplification.
Fifth, of the 223 informative samples among the 238 that we screened for Xp11.2 deletions, those with deletions encompassing the *FOXP3* locus had significantly higher HER-2 scores compared to those without deletions (P=0.03). Likewise, we compared the relative HER-2 scores among the 50 samples in which we had sequenced all *FOXP3* exons. As shown in Supplemental Table 5, the mutations in the FOXP3 gene correlated with higher levels of HER-2 (P=0.0083).

Significance

Our data demonstrated that we have reached the main goals of the project, namely identification of the target gene and genetic mechanism responsible for FoxP3 defect in human cancer. Our data provide strong evidence that FoxP3 is the first X-linked tumor suppressor gene in breast cancer and that its mutation and deletion can be responsible for a significant proportion of human breast cancer.

Publication

Tao Zuo, Lizhong Wang, Carl Morrison, Xing Chang, Huiming Zhang, Michael Chan, Xingluo Liu, Yan Liu, Yin Wang, Richard Love, Tim M Huang, Tianyu Yang, Pan Zheng and **Yang Liu.** The X-linked gene *Foxp*3 is an important suppressor gene for breast cancer and repressor of *Her-2/neu*/ErbB2. Cell (In revision).

FOXP3 is an X-linked breast cancer suppressor gene and an important repressor of the *HER-2/ErbB2* oncogene

Tao Zuo[1, 3, 4], Lizhong Wang[1,5], Carl Morrison[2], Xing Chang[1, 3, 5], Huiming Zhang[1, 5], Weiquan Li[5],Yan Liu[1, 5], Yin Wang[1, 5], Xingluo Liu[1], Michael W.Y. Chan[4], Jin-Qing Liu[1], Richard Love[6], Chang-gong Liu[4], Virginia Godfrey[7], Rulong Shen[2], Tim H-M. Huang[4], Tianyu Yang[1], Bae Keun Park[8], Cun-Yu Wang[8], Pan Zheng[1, 9] and Yang Liu[1, 5]

1. Division of Cancer Immunology

2. Department of Pathology

3. Program in Molecular, Cellular, and Developmental Biology

4. Department of Molecular Virology, Immunology and Medical Genetics
Ohio State University Medical Center and Comprehensive Cancer Center
Columbus, OH 43210 USA

5. Division of Immunotherapy, Department of Surgery, Program of Molecular Mechanism of Diseases, Cancer Center, University of Michigan,

6. Department of Internal Medicine, The Ohio State University, Columbus, OH 43210

7. Department of Pathology, University of North Carolina, Chapel Hill, NC 27599.

8. Laboratory of Molecular Signaling and Apoptosis, Department of Biologic and Materials Sciences, School of Dentistry, University of Michigan

9. Departments of Surgery and Pathology, Cancer Center and Program of Molecular Mechanisms of Disease, University of Michigan, Ann Arbor, MI 48109

#Correspondence: Drs. Yang Liu (Yangl@umich.edu) and Pan Zheng (panz@umich.edu)

Abstract

***A priori,* X-linked tumor suppressor genes would be of great interest as one allele of these genes might be silenced due to X-chromosome inactivation. The X-linked *Foxp3* is a member of the forkhead/winged helix transcription factor family. Germ-line mutations cause lethal autoimmune diseases in males. Serendipitously, we observed that *Foxp3*$^{sf/+}$ heterozygous mice developed cancer at a high rate. The majority of the cancers were mammary carcinomas in which the wild-type *Foxp3* allele was inactivated and *ErbB2* was over-expressed. Foxp3 bound and repressed the *ErbB2* promoter. Deletion, functionally significant somatic mutations and down-regulation of the *FOXP3* gene were commonly found in human breast cancer samples and correlated significantly with HER-2 over-expression, regardless of the status of *HER-2* amplification. *In toto*, the data demonstrate that *FOXP3* is an X-linked breast cancer suppressor gene and an important regulator of the *HER-2/ErbB2* oncogene.**

Introduction

Identification of *BRCA1* and *BRCA2* marks a key advance in understanding the genetic defects responsible for breast cancer (Miki, 1994; Wooster, 1995). Several other genes, such as *TP53, PIK3CA* and *PTEN*, have also been implicated in familial and sporadic cancers (Samuels et al., 2004; Wooster, 2003). However, the genetic defects for breast cancer remain to be fully elucidated. There is an important distinction between autosomal and X-linked genes, as many genes in the latter category are subject to X-inactivation, making it easier to fulfill Knudson's two-hit theory (Knudson, 1971). As such, X-linked tumor suppressor genes can potentially be more important, as LOH or mutation of a single allele can in effect functionally silence the gene (Spatz, 2004). However, essentially all tumor suppressor genes are autosomal (Spatz, 2004), although tantalizing evidence concerning abnormalities in the X-chromosome, including LOH, skewed inactivation and selective loss, has been reported in breast cancer samples (Kristiansen et al., 2005; Piao and Malkhosyan, 2002; Richardson et al., 2006; Roncuzzi et al., 2002).

In addition to tumor suppressor genes, oncogenes play a critical role in the development of cancer. *HER-2/Neu/ErbB2* is one of the first oncogenes to be identified (Schechter et al., 1984) and has been demonstrated to be expressed in a large proportion of cancer cells (Garcia de Palazzo et al., 1993). The level of HER-2/NEU is an important prognostic marker (Slamon et al., 1987). Anti-HER-

2/NEU antibody Herceptin has emerged as an important therapeutic for patients with over-expressed HER-2/NEU on cancer tissues (Slamon et al., 2001). As direct evidence for its involvement in the development of breast cancer, multiple lines of transgenic mice over-expressing HER-2/NEU in mammary epithelial cells develop mammary tumors with a high penetrance and rapid onset (Muller et al., 1998).

One of the most fascinating aspects of cancer biology is the interaction between tumor suppressor genes and oncogenes. Most of these interactions are mediated by post-translational modifications. On one hand, proteins encoded by tumor suppressor genes can inactivate oncogenes. One of the most clearly studied cases is tumor suppressor Rb that inhibits E2F family members of oncogenes (Nevins et al., 1997). Conversely, oncogenes can antagonize the tumor suppressor proteins. For example, SKP2 causes degradation of tumor suppressor FOXO (Muller et al., 1998), as well as CDK inhibitors, such as P27 (Carrano et al., 1999). It is less clear whether such antagonism exists at the transcriptional level. However, a recent study suggests that *FOXO* may repress expression of *cyclin D* (Schmidt et al., 2002), a well known oncogene.
Given the clinical and therapeutic significance of *Her-2/Neu/ErbB*2 over-expression (Garcia de Palazzo et al., 1993; Muller et al., 1998; Schechter et al., 1984; Slamon et al., 1987; Slamon et al., 2001), it is important to identify the molecular mechanisms responsible for the over-expression. A well established mechanism responsible for HER-2 over-expression in human cancer is gene amplification (Slamon et al., 1987). However, it is unclear whether gene

amplification alone is sufficient to cause HER-2 over-expression. Moreover, a significant proportion of human cancers with moderate over-expression of HER-2 do not show gene amplification (Bofin et al., 2004; Jimenez et al., 2000; Todorovic-Rakovic et al., 2005). It is therefore of great interest to identify regulators for *HER-2* expression in breast cancer. In this context, Xing et al. (Xing, 2000) reported that DNA-binding protein PEA3 specifically targets a DNA sequence on the *HER-2/neu* promoter and downregulates the promoter activity. Expression of PEA3 resulted in preferential inhibition of cell growth and tumor development of HER-2/neu-overexpressing cancer cells. It is less clear, however, whether genetic lesions of PEA3 can cause HER-2 over-expression.

Foxp3 is among the newest members of the forkhead winged helix family. It was identified during position cloning of *Scurfin*, a gene responsible for X-linked autoimmune diseases in mice and humans (Immune dysregulation, polyendopathy, enterophathy, X-linked, IPEX) (Bennett, 2001; Brunkow, 2001; Chatila, 2000; Wildin, 2001). The mutations in the mice and in some human IPEX patients are analogous as they cause frameshift and early termination of translation (Bennett, 2001; Brunkow, 2001; Chatila, 2000; Wildin, 2001). Further studies indicated that the gene is responsible for the development of regulatory T cells that suppress immune response (Fontenot, 2003), which partly explains the autoimmune phenotype of diseases. Surprisingly, in our analysis of the immune function of mice heterozygous for the Foxp3 mutation, we observed a high rate of spontaneous mammary cancer. We therefore systematically analyzed whether the *Foxp3* gene is a mammary tumor suppressor in mice and humans.

Moreover, mutation of the *Foxp3* leads to over-expression of *Her-2/ErbB2* in both mouse and human breast cancer. *Foxp3* represses the transcription of the *HER-2/ErbB2* gene via interaction with forkhead DNA binding motifs in the *ErbB2* promoter.

Results

Spontaneous and carcinogen-induced mammary cancer in *Foxp3$^{sf/+}$* female mice

Before the identification of the *scurfy* gene as *Foxp3*, the *scurfy* (*sf*) locus had been mapped in coupling and repulsion crosses to a location near the *sparse fur* (*spf*) locus, which encodes for ornithine transcarbamylase (OTC) (DeMars et al., 1976). The mutant BALB/c mice we used for the initial study thus carried mutations in two closely linked X-chromosome genes, *Foxp3^{sf}* and *Otc^{spf}*. During the course of the study, a spontaneous segregation of *Otc^{spf}* allowed us to obtain a BALB/c *Otc$^{spf/+}$* strain. Meanwhile, we obtained an independent line of Scurfy mice that had never been crossed to the *Spf* mutant mice and backcrossed the *Scurfy* mutant allele (*Foxp3^{sf}*) for more than 12 generations into the BALB/c background (Chang et al., 2005). Because of extensive backcross, the mice used in the study had the BALB/c allele of both *Prkdc* and *Cdkn2a*, which have been shown to facilitate the development of breast cancer (Blackburn et al., 2003; Yu et al., 2001). Female mice with only one copy of the *Foxp3* gene survived to adulthood and appeared normal within the first year of life (Godfrey et al., 1991) with normal T cell function (Fontenot et al., 2003; Fontenot et al., 2005;

Godfrey et al., 1994). The heterozygous mice and their WT littermates were used as breeders and were retired when they reached about one year of age. Our extended observations of the retired breeders for up to two years revealed that close to 90% of the *Foxp3*$^{sf/+}$*Otc*$^{spf/+}$ and *Foxp3*$^{sf/+}$ mice spontaneously developed malignant tumors. Cancer incidences in the littermate controls and a line of congenic mice with a mutation in *Otc* but not *Foxp3* were comparable with each other (Figure 1A, B). About 60% of the tumors were mammary carcinomas (Fig. 1A, C), although other tumors, such as lymphoma, hepatoma, and sarcoma were observed. Histological analyses revealed lung metastasis (Fig. 1A lower panels, based on expression of ER and/or PR, data not shown) in about 40% of the mice with mammary cancer. More than a third of the tumor-bearing mice had multiple lesions in the mammary glands. Most, although not all, mammary carcinomas expressed the estrogen receptor (ER$^+$, 14/18) and progesterone receptor (PR$^+$, 12/18).

In order to focus on mammary cancer, we treated the mice with a carcinogen, 7,12-dimethylbenz [a] anthracene (DMBA), in conjunction with progesterone, which resulted in an accelerated rate of mammary cancer in the BALB/c mice (Aldaz et al., 1996; Lydon et al., 1999). Mice heterozygous for *Foxp3*^{sf}, but not those heterozygous for *Otc*^{spf}, showed substantially increased susceptibility to mammary cancer, as revealed by earlier onset, increased incidence (Fig. 1D) and multiplicity (data not shown) of the breast tumors. These data demonstrate that a mutation of *Foxp3*, but not *Otc* results in a major increase in susceptibility to mammary carcinoma.

Foxp3 expression in normal and cancerous mammary tissues

Since expression of *Foxp3* has not been reported in mammary tissue, we isolated normal and cancerous cells by laser-capture microdissection (Supplemental Fig. S1A) and compared expression of *Foxp3* and *Otc* by real-time RT-PCR and histochemistry. The complete absence of the *cd3* transcripts (Fig. S1B) indicate that the micro-dissected samples were devoid of T cells, the main cell types known to express *Foxp3* (Fontenot et al., 2005). A representative profile and summarized data of *Foxp3* expression in $Foxp3^{sf/+}Otc^{spf/+}$ mice and age-matched *WT* control mice are shown in Fig. 2A. *Foxp3* mRNA was detected in normal mammary epithelium from both the WT and $Foxp3^{sf/+}Otc^{spf/+}$ mice, but not in mammary cancer cells from the same $Foxp3^{sf/+}Otc^{spf/+}$ mice. Immunohistochemical staining (Fig. 2B) confirmed the loss of expression of *Foxp3* in the mammary carcinoma generated from the $Foxp3^{sf/+}Otc^{spf/+}$ mice.

Foxp3 is an X-linked gene that is subject to X-chromosomal inactivation (Fontenot et al., 2005). The scurfy mutation is caused by the insertion of AA di-nucleotides resulting in a frameshift and early termination codon. It is therefore possible that the absence of *Foxp3* expression in mammary cancer cells is due to the X-chromosome inactivation of WT alleles, leaving the mutant allele active but unable to accumulate significant levels of *Foxp3* mRNA. To test this possibility, we carried out an anchored RT-PCR and cloned the low levels of *Foxp3* mRNA in the breast tissues. We sequenced the cDNA clones from pooled samples after ruling out potential T cell contamination (based on a lack of T-cell

specific *cd3* transcripts, Fig. S1B). As shown in Fig. 2C, right panel, 100% of the *Foxp3* transcripts in the cancerous tissues were from the mutant alleles, which indicate that the wild-type allele was silenced in the tumor cells. In contrast, the transcripts from the mutant allele constituted 15% of the transcripts in the normal mammary samples from the same mice. The under-representation of the mutant allele in normal tissue likely reflects the reduced mRNA stability of the mutant transcript rather than preferential silencing of the mutant allele. Thus, the expression pattern of *Foxp3* fulfills another criterion for a tumor suppressor gene.

FOXP3 **is a repressor of** ***ErbB2*** **transcription**

HER-2/ErbB2 over-expression is critical for the growth of multiple breast cancer cell lines and confers a poor prognosis in breast cancer patients (Slamon et al., 1987; van de Vijver et al., 1988). To understand the mechanism by which disruption of *Foxp3* promotes tumorigenesis, we analyzed the expression of *ErbB2* in the normal and cancerous mammary tissues. As shown in Figure 3A and supplemental Table S1, mammary cancer tissue from the $Foxp3^{sf/+}Otc^{spf/+}$ mice showed significant over-expression of ErbB2 as revealed by immunohistochemistry. Using real-time RT-PCR, 8-12-fold more *ErbB2* mRNA was found in the cancer cells than in normal epithelium (Fig. 3A). There was also more *ErbB2* mRNA in the $Foxp3^{sf/+spf/+}$ epithelium than in that of the *WT* female mice (Fig. 3A), which indicates a potential gene dosage effect of *Foxp3* on the regulation of *ErbB2* expression in vivo. Transfection of the TSA cell line with *Foxp3* cDNA repressed *ErbB2* levels on the TSA cell line (Fig. 3B).

Increased activity of the *Her-2/ErbB2* promoter plays an important role in the over-expression of this oncogene in breast cancer (Hurst, 2001; Scott, 2000; Xing, 2000). One potential mechanism by which *Foxp3* represses *Her-2/ErbB2* is to inhibit the promoter activity. As shown in Fig. 3C top panels, analysis of the 5' sequence of the *ErbB2* gene revealed multiple binding motifs for the forkhead domain. To test whether Foxp3 interacts with the *ErbB2* promoter, we used anti-V5 antibody to precipitate sonicated chromatin from the TSA cells transfected with the Foxp3-V5 cDNA and used real-time PCR to quantitate the amounts of the specific *ErbB2* promoter region precipitated by the anti-V5 antibodies in comparison to those that bound to mouse IgG control. As shown in Fig. 3C, the anti-V5 antibodies pulled down significantly higher amounts of *ErbB2* promoter DNA than the IgG control, with the highest signal around 1.6 kb 5' of the transcription starting site.

To test whether the binding correlated with the suppression by Foxp3, we produced luciferase reporter using the 1.8, 1.2 and 0.8 Kb upstream of the *ErbB2* TSS and tested the ability of Foxp3 to repress *ErbB2* promoter activity. In three separate cell lines, we observed that the region with the strongest ChIP signal was required for optimal repression by Foxp3 (Fig. 3D). Furthermore, we deleted two *Foxp3*-binding sites conserved between mouse and human (Supplemental Fig. S2) by site-directed mutagenesis and measured the effect on Foxp3-mediated repression. As shown in Fig. 3E, deletion of either binding site substantially increased the *ErbB2* promoter activity in the presence of Foxp3 and thus alleviated Foxp3-mediated repression.

Since mutant B also showed a significant reduction in basal promoter activity, it is theoretically possible that loss of suppression by Foxp3 may be linked to the loss of another enhancer. As such, Foxp3 may only indirectly affect the *ErbB2* promoter. To rule out this possibility, we first used an electrophoretic mobility shift assay (EMSA) to determine whether the forkhead DNA-binding motifs in region B bound to Foxp3. As shown in Fig. 3F, the nuclear extracts from the *Foxp3*-expressing cells specifically retarded migration of the WT but not mutant ^{32}P-labeled probes compared with control cells. Since our Foxp3 antibodies could not be used for the super-shift assay, we performed oligonucleotide competition analysis. While mutant cold probes did not affect Foxp3 binding activities, WT cold probes significantly diminished them, establishing that the binding of these complexes is specific to forkhead DNA-binding motifs. Based on these data, we carried out site-directed mutagenesis to replace the 12 nucleotides (mut C) within the *ErbB2* promoter and compared the promoter activity and Foxp3-repression by luciferase assays. As shown in Fig. 3G, while the wild-type promoter was repressed by Foxp3, no repression by Foxp3 was observed when the mutant promoter was used. Moreover, in contrast to the deletional Mut B, the mutations had no impact on the basal activity of the *ErbB2* promoter. Taken together, our new data make a compelling case that Foxp3 represses the ErbB2 promoter via specific forkhead binding motifs.

FOXP3 defects in human breast cancer

We analyzed the levels and isoforms of the *FOXP3* transcripts in a panel of normal human mammary epithelial cells (HMEC), an immortalized but non-malignant cell line (MCF-10A), and 10 malignant breast cancer cell lines differing in ER/PR and HER-2 status. As shown in Fig. 4A, similar levels of *FOXP3* transcripts were observed in two lines of HMEC and in the immortalized cell line MCF-10A. Each of the 10 tumor cell lines had a different degree of reduction in *FOXP3* mRNA levels in comparison to HMEC and MCF-10A. Among them, 2 were completely devoid of FOXP3 mRNA, while the others had a 1.5-20 fold reduction. We then used anchored primers spanning exons 1-12 to amplify the FOXP3 transcripts, and then we sequenced the PCR products. As shown in Fig. 4A, none of the tumor cell lines expressed full-length *FOXP3* transcripts. The HMEC expressed the same two isoforms as observed in the T cells, while MCF-10A expressed the exon 3-lacking isoform which was somewhat less functional than the full length FOXP3 in repressing proliferation of human T cells (Allan et al., 2005). The same isoform was also found in 4 tumor cell lines at much lower levels. In addition, 3 tumor cell lines expressed an isoform lacking both exons 3 and 4. The alternative splicing resulted in a frame-shift beginning at codon 70 and an early termination at codon 172. Furthermore, 2 tumor cell lines expressed a FOXP3 isoform lacking exons 3 and/or 8. Exon 8 encodes the leucine-zipper domain that is frequently mutated in IPEX patients (Ziegler, 2005). Thus, FOXP3 is abnormal in breast cancer cell lines. Consistent with a role for *FOXP3* in repressing *HER-2* expression, the majority of the breast cancer cell lines had higher levels of HER-2 in comparison to normal HMEC (Fig. 4A, lower

panel). However, additional changes are also likely required for *HER-2* over-expression, as three cell lines did not over express *HER-2* even though the *FOXP3* transcripts were greatly reduced.

We took three approaches to determine whether the findings in the mutant mice and human breast cancer cell lines are relevant to the pathogenesis of human breast cancer. First, we used immunohistochemistry to determine expression of FOXP3 in normal vs. cancerous tissue. As shown in Fig. 5A, while more than 80% of the normal breast samples expressed FOXP3 in the nuclei of the epithelial cells, less than 20% of the cancerous tissue showed nuclear staining. The difference between normal and cancerous tissue was highly significant ($P=6.0x10^{-16}$). Reduced expression of FOXP3 was observed among ER^+ ($P=1.0x10^{-7}$) and ER^- ($P=8.2x10^{-18}$) cancer samples, although more severe reduction was observed in the ER^- than in the ER^+ tumor group (P=0.002). RT-PCR revealed that the *FOXP3* transcripts in the primary human mammary epithelial cells (HMEC) contained two major forms that were found in human T cells (Allan et al., 2005).

Second, we used fluorescence in situ hybridization (FISH) to determine whether the *FOXP3* gene was deleted in the breast cancer samples. The minimal common region of deletion was identified using flanking p-telomeric and centromeric clones. Out of 223 informative samples, we observed 28 cases (12.6%) with deletions in any of the three loci. Interestingly, deletion of the *FOXP3* locus was found in all of the 28 cases (Fig. 5B and supplemental Table S2). These data suggest that *FOXP3* is likely within the minimal region of

deletion in the Xp11 region studied. Although all deletions were heterozygous (data not shown), the FOXP3 protein was undetectable in 26/28 cases. Thus, it appears that for the majority of the breast cancer samples, LOH alone was sufficient to inactivate the locus, perhaps due to X-chromosomal inactivation. The two cases with both deletion and FOXP3 expression had X-polysomy with 3 and 4 X-chromosomes respectively (Table S2).

Thirdly, we isolated DNA from matched normal and cancerous tissues (50 cases with formalin fixed samples and 15 cases of frozen samples) from patients with invasive ductal carcinoma and amplified all 11 coding exons and intron-exon boundary regions by PCR. Two independent PCR products were sequenced in order to confirm the mutations. Unless the bulk sequencing data were unambiguous (Fig. 5C top panel and Supplemental Fig S3a & c), the PCR products were cloned and 5-10 independent clones from each reaction were sequenced (Supplemental Fig. S3b). Among the formalin fixed samples, we only used the cases in which the normal tissue samples gave unambiguous sequencing data that matched the wild-type *FOXP3* sequence. When the cancerous tissues were compared with normal tissues from the same patient, 36% (18/50 formalin-fixed samples and 5/15 frozen samples) showed somatic mutations (Table S3). Loss of wild-type allele was found in 6/23 cases (38%) of cancer samples with somatic *FOXP3* mutations (See Fig. 5C for an example). The other cases had heterozygous mutation (Supplemental Fig. S3a). Eighteen mutations resulted in the replacement of amino acids in domains. Most are likely to be critical for FOXP3 function, as judged from the pattern of mutation in IPEX

patients (Ziegler, 2005) or in the conserved zinc finger domain that has so far not been implicated (Fig. 5D).

Although most samples had a single mutation of the *FOXP3* gene, we did observed two cases with multiple mutations. In the first sample (supplemental Fig S3b, case 3 in Table S3), the two mutations occurred in consecutive codons, resulting in two nonconservative replacements of amino acid residues. Clonal analysis revealed that both mutations occurred in the same clone (Fig. S3b). In the second sample (Table S3, case 16), three mutations occurred in intron 11. Since this case lacked a WT allele (Supplemental Fig. 3c), it is likely that all of the mutations occurred in the same allele. The possibility of a mismatch in the cancer and normal samples was ruled out by comparing the normal and cancer samples for polymorphism of two unrelated genes. One was the *CD24* gene in chromosome 6 and the other was the X-linked *OTC* gene (data not shown).

To directly test whether FOXP3 mutations affect the repressor activity for the *HER-2* gene, we chose two representative somatic *FOXP3* mutants isolated in the cancer cells and tested their repressor activity for the *HER-2* promoter. One mutation (338P>L) resided in the signature forkhead domain which is often mutated in the IPEX patient, while the other double mutation (*204C>R205E>K*) was from the zinc finger domain that has not been implicated in IPEX patients. As shown in Fig. 5F, both mutations significantly reduced the repressor activity of FOXP3. The reduced repression of the *HER-2* promoter correlates with a significantly reduced inhibition of *HER-2* mRNA (Fig. 5E).

Four cases had mutations in introns that may potentially affect RNA splicing. We used laser-guided micro-dissection to isolate normal and cancerous epithelial cells from one case with a mutation in intron 6 (case 23, Supplemental Table S3). RNA was isolated and tested for the potential effect of the mutation on RNA splicing (using primers on exons 5 and 8) and total *FOXP3* transcript, as quantitated by real time PCR using primers spanning exons 10-12. Tissues from another patient with a mutation in exon 7 were used as control. As show in Fig. 5F upper panel, primers spanning exons 5 and 8 failed to detect *FOXP3* mRNA from the cancerous tissue of case No. 23. Furthermore, primers spanning exons 10-12 also failed to detect any *FOXP3* transcripts. Substantial levels were detected in the normal epithelial cells of the same patients as well as in normal and cancerous tissues from case No. 22. Since the wild-type allele had been lost in the cancer cells of case No. 23, it is likely that the mutation in intron 6 inactivated *FOXP3.* With an intron of 944 nucleotides, a mutation that prevented splicing of intron 6 would cause premature-termination codon-mediated RNA decay, which is operative in the *FOXP3* gene (Chatila et al., 2000).

These data demonstrate that the *FOXP3* locus is targeted in breast cancer by a number of different mechanisms, including deletion, somatic mutation and other unknown mechanisms of silencing. Since the samples used for mutational analysis are limited and do not completely overlap with those used for FISH, it is unclear whether these two mechanisms act in concert to inactivate the *FOXP3* locus.

FOXP3 defects and HER-2 over-expression

We have obtained five lines of evidence that support a critical role for *FOXP3* in the repression of the *HER-2* oncogene in human breast cancer. First, we silenced the *FOXP3* gene in primary HMEC using a lentiviral vector expressing *FOXP3* siRNA. As shown in Fig. 6A, the *FOXP3* siRNA reduced *FOXP3* expression by more than 100-fold while increasing *HER-2* mRNA by 7-fold. A corresponding increase in cell surface HER-2 was also observed (Fig. 6B). These results implicate *FOXP3* as a repressor of *HER-2* in human breast epithelial cells.

Second, since a major mechanism for HER-2 up-regulation in breast cancer is gene amplification (Kallioniemi et al., 1992), an intriguing issue is whether *FOXP3* is capable of repressing HER-2 in cancer cells with an amplified HER-2 gene. We produced a Tet-off line of BT474, a breast cancer cell line known to have HER-2 gene amplification (Kallioniemi et al., 1992), and transiently transfected it with a *pBI-EGFP-FOXP3*- vector. After drug selection, the cells were cultured either in the presence or absence of doxycycline. While the cells cultured with doxycycline did not express FOXP3 (data not shown), removal of doxycycline resulted in induction of FOXP3 in a significant fraction of the cancer cells, which allowed us to compare HER-2 levels in the $FOXP3^+$ and $FOXP3^-$ cells in the same culture by flow cytometry. As shown in Fig. 6C, $FOXP3^-$ cells had about a 5-10-fold higher level of HER-2 protein on the cell surface in comparison to the $FOXP3^+$ cells. These results, together with the data

in Fig. 5E involving SKBr3, demonstrate that FOXP3 can suppress HER-2 expression even in cells with multiple copies of the HER-2 gene.

Thirdly, we compared the expression of FOXP3 with HER-2 expression in breast cancer tissues. As shown in Fig. 6D, down-regulation of FOXP3 was strongly associated with the over-expression of HER-2, which supports a role for *FOXP3* inactivation in *HER-2* over-expression in breast cancer. Nevertheless, since many of the $FOXP3^-$ cells remained $HER\text{-}2^-$, it is likely that dis-regulation of *FOXP3* is insufficient for *HER-2* up-regulation. On the other hand, since only 3/82 $FOXP3^+$ cancer cells expressed high levels of HER-2, *FOXP3* inactivation is likely important for *HER-2* up-regulation under most circumstances.

Fourth, we divided breast cancer samples based on their *HER-2* gene copy numbers and compared the $FOXP3^+$ and $FOXP3^-$ cancer samples for the relative amounts of cell surface HER-2 expression. As shown in Fig. 6E, in each of the gene dose categories, $FOXP3^+$ samples had reduced HER-2 scores in comparison to the $FOXP3^-$ samples. These results strongly suggest a critical role for FOXP3 in repressing HER-2 expression even in the cases of the *HER-2* gene amplification.

Fifth, of the 223 informative samples among the 238 that we screened for Xp11.2 deletions, those with deletions encompassing the *FOXP3* locus had significantly higher HER-2 scores compared to those without deletions (P=0.03) (Supplemental Table 4). Likewise, we compared the relative HER-2 scores among the 50 samples in which we had sequenced all *FOXP3* exons. As shown

in Supplemental Table 5, the mutations in the FOXP3 gene correlated with higher levels of HER-2 (P=0.0083).

Foxp3/FOXP3 inhibits tumorigenicity of breast cancer cells

To test whether the *Foxp3* gene can suppress the growth of breast cancer cells, we transfected the empty vector or the vectors carrying either *Foxp3* (mouse or human origin) or *Otc* cDNA into three breast cancer cell lines, including mouse mammary tumor cell line TSA or human breast cancer cell lines MCF7 ($ER^+HER\text{-}2^{low}$, no *HER-2* amplification) and SKBr3 ($ER^-HER\text{-}2^{high}$ with *HER-2* amplification). Since all vectors carried a neomycin-resistance gene, the untransfected cells were removed by a selection with G418. The numbers of drug-resistant cells were comparable among different groups initially, which suggests comparable transfection efficiency. However, while the vector-transfected cells grew rapidly, the *Foxp3*-transfected cell lines seldom grew into large colonies. The *Foxp3*-transfected culture had a drastic reduction in both the size and the number of the drug-resistant colonies. No effect was observed when the *Otc* cDNA was used (Fig. 7A&B). Similar growth inhibition was found in BT474, another human breast cancer cell line with *HER-2* amplification (Kallioniemi et al., 1992) (data not shown).

To test whether the somatic mutations uncovered from cancerous tissues ablated their growth inhibition, we transfected WT and two mutant Foxp3 cDNA into SKBr3 and MCF7 cell lines. As shown in Fig. 7C, in both cell lines, the mutants had greatly reduced ability to suppress tumor growth.

An intriguing issue is whether repression of *ErbB2* explains the tumor suppressor activity of the *Foxp3* gene in the ErbB2^{+} cancer cell line. We transfected TSA cells with mouse CMV promoter-driven *ErbB2* cDNA cloned into the pcDNA6 vector and evaluated their susceptibility to *Foxp3*-mediated growth suppression. In this setting, the expression of *ErbB2* was resistant to *Foxp3*-mediated repression (data not shown). If repression of endogenous *ErbB2* is critical for *Foxp3*-mediated tumor suppression, ectopic expression of *ErbB2* should alleviate the growth inhibition by *Foxp3*. As shown in Fig. 7D & E, while the pcDNA6-vector-transfected TSA cells remained susceptible to *Foxp3*-mediated repression, the *ErbB2*-transfected TSA cells were completely resistant. In contrast, transfection of *c-Myc* barely alleviated the growth inhibition by *FOXP3* (Fig. 7E). These results suggest that *Foxp3* suppresses TSA growth by repressing transcription of *ErbB2*.

We transfected TSA cells with either empty vector or V5-tagged *Foxp3* cDNA. The stable transfectant cell lines were selected by G-418. The vector and *Foxp3-V5*-transfected cell lines were injected into syngeneic BALB/c mice, which were then observed for tumor growth and mouse survival. As shown in Fig. 7F, *Foxp3*-transfectants showed reduced growth in vivo. The mice that received TSA-Vector cells became moribund earlier with higher incidence, while about 50% of the mice that received the *Foxp3-V5*-transfected cells survived more than 7 weeks (Fig. 7G). Similarly, *Foxp3*-transfected 4T1, a mouse mammary cancer cell line with *ErbB2* over-expression, also showed reduced tumorigenicity in vivo (data not shown).

Discussion

Foxp3 is an X-linked mammary tumor suppressor gene

Foxp3 encodes the transcription factor identified because of its role in autoimmune diseases in mouse and man (Bennett, 2001; Brunkow, 2001; Chatila, 2000; Wildin, 2001). In our analysis of the immune function of *Foxp3*, we made an unexpected observation that mice heterozygous for the *Foxp3* mutation spontaneously developed mammary cancer at a high rate. Although the initial observation was made in mice that carried mutations of both *Foxp3* and a closely linked *Otc* gene, we have subsequently reproduced the observation with a completely independent line of BALB/c mice that were crossed to *Foxp3* heterozygous founder mice with a WT *Otc* locus. Since two independently maintained lines sharing the *Foxp3* mutation have a comparably higher incidence of mammary cancer, the *Foxp3* mutation is likely responsible for the increased rate of breast cancer. It should be noted that the $Foxp3^{sf/+}$ founder mice have been continuously bred to WT BALB/c mice for at least 12 generations, and many of the data are from mice with more than 20 generations of backcross. The independent confirmation and long backcross have made it virtually impossible to explain the increased cancer susceptibility by mutations other than those in the *Foxp3*-linked gene. Since surrounding open-reading frames in the original founder mice have all been confirmed to be normal during position

cloning of *Foxp3* (Brunkow et al., 2001), we conclude that the *Foxp3* mutation is responsible for the cancer phenotype, as described herein.

Unlike essentially all cancer suppressor genes identified to date, *Foxp3* is X-linked and is known to be subjected to X-chromosomal inactivation (Fontenot et al., 2005). As such the *Foxp3* locus can be regarded as operational loss of heterozygocity (LOH). In this scenario, inactivation of the *Foxp3* locus can be achieved in heterozygous mice by silencing the WT allele. This is indeed the case as the low levels of *Foxp3* transcripts in the cancer cells were derived exclusively from the mutant alleles. It is feasible that in animals with two wild-type alleles, somatic mutation or LOH of the allele in the active chromosome will increase the risk of breast cancer.

The spontaneous cancer observed in the heterozygous mice are predominantly but not exclusively of mammary origin. Thus, the tumor suppressor activity is not limited to mammary tissue. This is not unexpected as mutations of most cancer suppressor genes, including the prototype *BRCA1,* can increase the risk of multiple lineages of cancers (Struewing et al., 1997). On the other hand, since *Foxp3* is known to be a master regulator for the development and function of regulatory T cells (Fontenot, 2003; Hori, 2003; Khattri, 2003), a natural question is whether the increased cancer risk is due to defective immune response. We consider it unlikely for two reasons. First, regulatory T cells act in a dominant fashion, and one functional *Foxp3* has been shown to be adequate to control immune response. Second, since regulatory T cells dampen cancer immunity (Onizuka et al., 1999; Sutmuller et al., 2001), inactivation of this cell

type should, in theory, enhance rather than suppress cancer immunity and would thus not explain the increased cancer risk.

Our analysis of human breast cancer samples provides strong support for an important role for the *FOXP3* gene in the development of breast cancer. First, we searched X chromosomal deletion using three markers encompassing more than 10MB of Xp11. Among 223 informative samples, we observed deletions in 28 cases. Most importantly, while the deletions varied in size, every single case with deletion in this region had a deleted FOXP3 gene. Thus *FOXP3* is likely the minimal region of deletion.

Second, we analyzed the *FOXP3* exons and some adjacent intronic sequences using both normal and cancerous tissues from the same individual. This analysis revealed a high proportion of somatic mutations in the FOXP3 gene (23/65 cases over about 2,000 bp exon and intron sequence scanned). The significance of our finding can be discerned indirectly based on the fact that the mutations tended to cluster around important domains, such as the FKH and the zinc finger domains. In addition, most of the mutations resulted in the non-conservative replacement of amino acids, and cancers with mutations identified had higher levels of HER-2 than those without mutations. The rate of missense to synonymous mutation was 18/3, which greatly exceeds what would be predicted if the mutations were not relevant to tumor development. More importantly, we demonstrated that two tested mutations in the FKH and zing finger domains inactivated the repressor activity and tumor growth inhibition, and that cancer tissues bearing an intronic mutation had an inactive *FOXP3* locus.

Moreover, mutations and deletions of *FOXP3* locus corresponded to increased HER-2 levels. These functional data strengthen the conclusion that the mutation of *FOXP3* is an important part of breast cancer pathogenesis.

Third, using affinity purified anti-FOXP3 antibodies whose binding to tissues depends on functional *Foxp3* gene (Chang et al., 2005), we have documented extensive down-regulation of FOXP3 among more than 600 cases of breast cancer tissues. Thus, approximately 80% of the normal breast sections tested were $FOXP3^{+}$, while only 20% of the cancer tissue sections expressed FOXP3. The down regulation was observed regardless of ER or PR expression among the cancerous tissues. The widespread down regulation is consistent with a general function of FOXP3 in repressing breast cancer.

Foxp3 **is a major transcriptional repressor for** ***ErbB2***

Her-2/Neu/ErbB2 is a major breast cancer oncogene and therapeutic target for human breast cancer (Garcia de Palazzo et al., 1993; Muller et al., 1998; Schechter et al., 1984; Slamon et al., 1987; Slamon et al., 2001). Its over-expression indicates a poor prognosis (Slamon et al., 1987). The molecular lesions leading to over-expression, however, remain poorly understood. A major contributing factor is the amplification of the *HER-2/Neu* locus, although it is unclear whether other alteration is needed to achieve over-expression. In addition, not all cancer cells with *HER-2* over-expression show gene amplification (Bofin et al., 2004; Jimenez et al., 2000; Todorovic-Rakovic et al., 2005). An intriguing possibility is the defective expression of potential *HER-2* repressors.

Recently, one such repressor, *PEA3*, was reported by Xing et al. (Xing, 2000). However, while PEA3 is capable of binding to the *HER-2* promoter region and repressing its expression, it is less clear whether defects in *PEA3* are responsible for HER-2 over-expression. Here we showed that the *Foxp3* mutation resulted in over-expression of *ErbB2*, the murine homologue of *HER-2*. In addition, transfection of *Foxp3* repressed *ErbB2* transcription. More importantly, chromatin immunoprecipitation and gel-shift analyses revealed that Foxp3 binds specifically to its consensus sequence in the 5' of the *ErbB2* gene. Since specific mutations in the promoter abrogate its susceptibility to repression by Foxp3, such binding is likely responsible for it.

Importantly, we have demonstrated that, for TSA cell line which has ErbB2 over-expression, the tumor suppressive effect of the *Foxp3* gene can be overcome by ectopic expression of the *ErbB2* cDNA, but not c-Myc cDNA. Thus, repressing the *ErbB2* locus is responsible for Foxp3's tumor suppressor activity for this *ErbB2* over-expressing cell line. The requirement for continuous expression of *ErbB2* is best explained by the concept of oncogene addiction, as proposed by Weinstein (Weinstein, 2002),

It should be noted that FOXP3 can also suppress the growth of tumor cell lines that do not grossly over-express *HER-2/ErbB2*, such as MCF-7. It is therefore likely that FOXP3 may suppress tumor growth by multiple mechanisms. In an effort to identify other potential FOXP3 targets, we have produced a FOXP3-Tet-off MCF-7 cell line that expresses FOXP3 upon removal of tetracycline (Fig. S4a). Using the most current version of Entrez Gene-based

CDFs for a more accurate GeneChip analysis (Dai et al., 2005), we uncovered wide-spread changes in the expression of genes that are involved in several pathways critical for cancer cell growth (Fig. S4b). Interestingly, 10 genes involved in ErbB2 signaling pathway were repressed by FOXP3 (Fig. S4c). Thus, multiple oncogenes can potentially be up-regulated by *FOXP3* inactivation. Because of oncogene addiction, however, different cancers can be dependent on different oncogenes.

We have obtained substantial evidence for the notion that *FOXP3* is an important transcriptional repressor of HER-2 in human breast tissues. First, silencing the *FOXP3* locus with siRNA enhanced expression of HER-2 in normal human mammary epithelial cell lines. Thus, FOXP3 acts as an endogenous repressor of *HER-2* in untransformed cells. Second, we have demonstrated that genetic lesions of *FOXP3*, including deletion, somatic mutation and other unidentified mechanisms, result in increased levels of HER-2. Thirdly, even among the cases with *HER-2* gene amplification, $FOXP3^{+}$ cancer had lower levels of HER-2. Finally, two somatic mutants found in breast cancer tissue have greatly reduced repressor activity.

Taken together, we have demonstrated that *FOXP3* is the first X-linked breast cancer suppressor that represses the *HER-2/ErbB2* oncogene. Given the significant role of HER-2 in the pathogenesis of human breast cancer and the

wide-spread defects of the *FOXP3* locus, it is likely that *FOXP3* is an important suppressor for human breast cancer.

Experimental Procedures

Materials Human mammary epithelial cells (HMEC-1, Cat# CC-2551) and mammary epithelial cell growth medium (MEGM Cat# CC-3051) were purchased from Cambrex Clonetics™. HMEC-2 was produced using the same protocol. TSA is an aggressive and poorly immunogenic cell line established from the first *in vivo* transplant of a moderately differentiated mammary adenocarcinoma that arose spontaneously in a BALB/c mouse (Giovarelli et al., 1995). Human breast cancer cell lines, MCF-7, SKBr3, BT474, MDA-MB-231, ZR75-1, T47D, BT549, BT20, MDA-MB468, MDA-MB453, mouse breast cancer cell line 4T1 and immortalized but non-malignant breast epithelial cell line MCF-10A were purchased from ATCC (Manassas, VA, USA).

The normal and cancerous breast tissues were obtained from the Ohio State University Department of Pathology Tissue Bank, Zymed Laboratories Inc (San Francisco, CA, USA), and US Biomax, Inc. (Rockville, MD, USA). Additional tissue microarray samples were prepared from breast cancer patient cohorts described in recent studies (Love et al., 2002; Love et al., 2003). Affinity purified rabbit anti-Foxp3 antibodies, specific for FOXP3 N-terminus peptide starting at position 25: (C)LLGTRGSGGPFQGRDLRSGAH, which is 80% conserved between mouse and man, were provided by Dr. Lishan Su from the University of North Carolina (Chapel Hill, NC, USA) (Chang et al., 2005). Other

antibodies were purchased from the following vendors: Santa Cruz Biotechnology, Inc. (Santa Cruz, CA, USA): ERα (MC-20), PRα (C-19), ErbB2 (C-18), and normal rabbit IgG. Dako (Carpinteria, CA, USA): HER-2/NEU (A0485). The *Scurfy* female mice with either two (*Foxp3*$^{sf/+}$*Otc*$^{spf/+}$) or one (*Foxp3*$^{sf/+}$) mutations were backcrossed to the BALB/c background for at least 12 generations at The University of North Carolina at Chapel Hill. *Sparse-fur* (*Otc*$^{spf/+}$) female mice used for the studies were obtained from the double mutant mice after a rare re-segregation of the two mutations at The Ohio State University Laboratory Animal Facility. Littermates of the mutants were used as control.

Quantitative real-time PCR Relative quantities of mRNA expression were analyzed using real-time PCR (Applied Biosystems ABI Prism 7700 Sequence Detection System, Applied Biosystems). The SYBR (Qiagen) green fluorescence dye was used in this study. The primer sequences (5'-3') were as follows: *Foxp3* forward: ATCTCCTGGATGAGAAAGGCAAGG, and reverse: TGTTGTGGAAGAACTCTGGGAAGG ; *Hprt* forward:AGCCTAAGATGAGCGCAAGT and reverse: TTACTAGGCAGATGGCCACA; *ErbB2* forward: AAACCTGGAACTCACCTACCTGC, and reverse: GGTATTGTTCAGCGGGTCTCCATT. murine cytokeratin 19, forward 5' -ACCCTCCCGAGATTACAACC-3', reverse 5' -CAAGGCGTGTTCTGTCTCAA-3'.

murine cd3ζ, forward 5' -TCTGCTGGATCCCAAACTCT-3',

reverse 5' -TGCACTCCTGCTGAATTTTG-3'.

HER-2 forward: 5'-ACCGGCACAGACATGAAGCT-3'; and reverse: 5'-AGGAAGGACAGGCTGGCATT-3'

FOXP3 forward: 5'-TACTTCAAGTTCCACAACATGCGACC-3' and reverse, :5'-CGCACAAAGCACTTGTGCAGACTCAG-3'.

The data were collected and analyzed by the ABI Prism 7700 sequence detection system software. Additional primers for the ChIP assays are available upon request.

Chromatin immunoprecipitation was carried out according to a published procedure (Im et al., 2004). Briefly, the Foxp3-V5-transfected TSA cells were sonicated and fixed with 1% paraformaldehyde. The anti-V5 antibodies or control mouse IgG were used to pull down chromatin associated with Foxp3-V5. The amounts of the specific DNA fragment were quantitated by real-time PCR and normalized against the genomic DNA preparation from the same cells.

***FOXP3*-silencing lentiviral vector**

The lentivirus-based siRNA expressing vectors were created by introducing the murine U6 RNA polymerase III promoter and a murine phosphoglycerate kinase promoter (pGK)-driven EGFP expression cassette into a vector of pLenti6/V5-D-TOPO back bone without CMV promoter. A hairpin siRNA sequence of *FOXP3* (target sequence at the region of 1256 to 1274 nucleotides; 5'-

GCAGCGGACACTCAATGAG-3') was cloned into the lentiviral siRNA expressing vectors by restriction sites of *Apa*I and *EcoR*I.

Immunohistochemistry and Fluorescence In-situ Hybridization (FISH)

HER-2 expression was performed using Pathway™ HER-2 (Clone CB11) (Ventana Medical Systems, Inc., Tucson, AZ) on the BenchMark® XT automated system per the manufacturer's recommended protocol. The HER-2 levels were scored by commonly used criteria (Yaziji et al., 2004). -, no staining on the membrane or membrane staining in less than 10% of the tumor cells, scored 0; faint perceptible membrane staining in more than 10% of the tumor cells was scored as 1 (+); weak to moderate complete membrane staining in more than 10% of the tumor cells was defined as ++, scored 2; the strong complete membrane staining in more than 10% of the tumor cells was defined as +++, scored 3. Three representative cases and summary data from 662 independent cases are presented.

FISH for FOXP3 deletion was done using BAC clone RP11-344O14 (ntLocus X: 48,817,975- 48,968,223), which was verified by PCR to contain the FOXP3 gene. The minimal common region of deletion was done using flanking p-telomeric and centromeric clones, RP11-573N21 (ntLocus X: 43,910,391-44,078,600) and RP11-353K22 (ntLocus X: 54,416,890- 54,545,788), respectively. Locus specific BAC clones were labeled with spectrum orange using commercially available reagents per the manufacturer's recommendations (Vysis, Downers Grove, Ill.). Chromosome X enumeration was done by FISH

using a commercially available spectrum green CEPX probe (Vysis, Downers Grove, Ill.). All FISH were done using standard protocols optimized for breast cancer specimens.

EMSA. Nuclear extracts were prepared as described previously (Wang et al., 1999). 10-μg aliquots of cell nuclear extracts were pre-incubated with 1 μg of poly(dI-dc) in binding buffer (10 mM Tris [pH 7.7], 50 mM NaCl, 20% glycerol, 1 mM dithiothreitol [DTT], 0.5 mM EDTA) for 10 min at room temperature. Approximately 1.5 x 10^4 cpm of ^{32}P-labeled DNA probes were then added and the reaction proceeded for 30 min. The sequence for the WT probe (W) was AGTTCAATTTGAATTTCAGATAAACG. Mutant probe (M) (AGTTCAGCGCGAGCGCCAGAGCGCCG) with mutations of all three potential forkhead binding sites was used as specificity control. The specificity of the binding was further confirmed by competition with a 50-fold excess of unlabeled probes. The complexes were resolved on a 5% polyacrylamide gel in Tris-glycine buffer consisting of 25 mM Tris, 190 mM glycine, and 1 mM EDTA at room temperature. The gel was dried at 80^{o}C for 60 min and exposed to an X-ray film.

Acknowledgement

We thank Dr. Fan Meng for assistance in bioinformatics, Drs. Eric Fearon, Albert de la Chapelle, Zhaohui Qin, Michael Caligiuri, Alexander Rudensky, and Charis

Eng for their valuable discussions and/or critical reading of the manuscript and Lynde Shaw for secretarial assistance. This study is supported by grants from the National Institutes of Health and the Department of Defense.

References

Aldaz, C.M., Liao, Q.Y., LaBate, M., and Johnston, D.A. (1996). Medroxyprogesterone acetate accelerates the development and increases the incidence of mouse mammary tumors induced by dimethylbenzanthracene. Carcinogenesis *17*, 2069-2072.

Allan, S.E., Passerini, L., Bacchetta, R., Crellin, N., Dai, M., Orban, P.C., Ziegler, S.F., Roncarolo, M.G., and Levings, M.K. (2005). The role of 2 FOXP3 isoforms in the generation of human CD4+ Tregs. J Clin Invest *115*, 3276-3284.

Bennett, C.L., Christie, J., Ramsdell, F., Brunkow, M.E., Ferguson, P.J., Whitesell, L., Kelly, T.E., Saulsbury, F.T., Chance, P.F., Ochs, H.D.. (2001). The immune dysregulation, polyendocrinopathy, enteropathy, X-linked syndrome (IPEX) is caused by mutations of FOXP3. Nat Genet *27*, 20-21.

Blackburn, A.C., Brown, J.S., Naber, S.P., Otis, C.N., Wood, J.T., and Jerry, D.J. (2003). BALB/c alleles for Prkdc and Cdkn2a interact to modify tumor susceptibility in Trp53+/- mice. Cancer Res *63*, 2364-2368.

Bofin, A.M., Ytterhus, B., Martin, C., O'Leary, J.J., and Hagmar, B.M. (2004). Detection and quantitation of HER-2 gene amplification and protein expression in breast carcinoma. Am J Clin Pathol *122*, 110-119.

Brunkow, M.E., Jeffery, E.W., Hjerrild, K.A., Paeper, B., Clark, L.B., Yasayko, S.A., Wilkinson, J.E., Galas, D., Ziegler, S.F., and Ramsdell, F. (2001). Disruption of a new forkhead/winged-helix protein, scurfin, results in the fatal lymphoproliferative disorder of the scurfy mouse. Nat Genet *27*, 68-73.

Brunkow, M.E., Jeffery, E.W., Hjerrild, K.A., Paeper, B., Clark, L.B., Yasayko, S.A., Wilkinson, J.E., Galas, D., Ziegler, S.F., Ramsdell, F.. (2001). Disruption of a new forkhead/winged-helix protein, scurfin, results in the fatal lymphoproliferative disorder of the scurfy mouse. Nat Genet *27*, 68-73.

Carrano, A.C., Eytan, E., Hershko, A., and Pagano, M. (1999). SKP2 is required for ubiquitin-mediated degradation of the CDK inhibitor p27. Nat Cell Biol *1*, 193-199.

Chang, X., Gao, J.X., Jiang, Q., Wen, J., Seifers, N., Su, L., Godfrey, V.L., Zuo, T., Zheng, P., and Liu, Y. (2005). The Scurfy mutation of Foxp3 in the thymus stroma leads to defective thymopoiesis. J Exp Med *202*, 1141-1151.

Chatila, T.A., Blaeser, F., Ho, N., Lederman, H.M., Voulgaropoulos, C., Helms, C., and Bowcock, A.M. (2000). JM2, encoding a fork head-related protein, is mutated in X-linked autoimmunity-allergic disregulation syndrome. J Clin Invest *106*, R75-81.

Chatila, T.A., Blaeser, F., Ho, N., Lederman, H.M., Voulgaropoulos, C., Helms, C., Bowcock, A.M.. (2000). JM2, encoding a fork head-related protein, is mutated in X-linked autoimmunity-allergic disregulation syndrome. J Clin Invest *106*, R75-81.

Dai, M., Wang, P., Boyd, A.D., Kostov, G., Athey, B., Jones, E.G., Bunney, W.E., Myers, R.M., Speed, T.P., Akil, H., *et al.* (2005). Evolving gene/transcript definitions significantly alter the interpretation of GeneChip data. Nucleic Acids Res *33*, e175.

DeMars, R., LeVan, S.L., Trend, B.L., and Russell, L.B. (1976). Abnormal ornithine carbamoyltransferase in mice having the sparse-fur mutation. Proc Natl Acad Sci U S A *73*, 1693-1697.

Fontenot, J.D., Gavin, M.A., and Rudensky, A.Y. (2003). Foxp3 programs the development and function of CD4+CD25+ regulatory T cells. Nat Immunol *4*, 330-336.
Fontenot, J.D., Gavin, M.A. and Rudensky, A.Y.. (2003). Foxp3 programs the development and function of CD4+CD25+ regulatory T cells. Nat Immunol *4*, 330-334.
Fontenot, J.D., Rasmussen, J.P., Williams, L.M., Dooley, J.L., Farr, A.G., and Rudensky, A.Y. (2005). Regulatory T cell lineage specification by the forkhead transcription factor foxp3. Immunity *22*, 329-341.
Garcia de Palazzo, I., Klein-Szanto, A., and Weiner, L.M. (1993). Immunohistochemical detection of c-erbB-2 expression by neoplastic human tissue using monospecific and bispecific monoclonal antibodies. Int J Biol Markers *8*, 233-239.
Giovarelli, M., Musiani, P., Modesti, A., Dellabona, P., Casorati, G., Allione, A., Consalvo, M., Cavallo, F., di Pierro, F., De Giovanni, C., *et al.* (1995). Local release of IL-10 by transfected mouse mammary adenocarcinoma cells does not suppress but enhances antitumor reaction and elicits a strong cytotoxic lymphocyte and antibody-dependent immune memory. J Immunol *155*, 3112-3123.
Godfrey, V.L., Rouse, B.T., and Wilkinson, J.E. (1994). Transplantation of T cell-mediated, lymphoreticular disease from the scurfy (sf) mouse. Am J Pathol *145*, 281-286.
Godfrey, V.L., Wilkinson, J.E., Rinchik, E.M., and Russell, L.B. (1991). Fatal lymphoreticular disease in the scurfy (sf) mouse requires T cells that mature in a sf thymic environment: potential model for thymic education. Proc Natl Acad Sci U S A *88*, 5528-5532.
Hori, S., Nomura, T., Sakaguchi, S.. (2003). Control of regulatory T cell development by the transcription factor foxp3. Science *299*, 1057-1061.
Hurst, H.C. (2001). Update on HER-2 as atarget for cancer therapy the ERBB2 promoter and its exploitation for cancer treatment. Breast Cancer Res *3*, 395-398.
Im, H., Grass, J.A., Johnson, K.D., Boyer, M.E., Wu, J., and Bresnick, E.H. (2004). Measurement of protein-DNA interactions in vivo by chromatin immunoprecipitation. Methods Mol Biol *284*, 129-146.
Jimenez, R.E., Wallis, T., Tabasczka, P., and Visscher, D.W. (2000). Determination of Her-2/Neu status in breast carcinoma: comparative analysis of immunohistochemistry and fluorescent in situ hybridization. Mod Pathol *13*, 37-45.
Kallioniemi, O.P., Kallioniemi, A., Kurisu, W., Thor, A., Chen, L.C., Smith, H.S., Waldman, F.M., Pinkel, D., and Gray, J.W. (1992). ERBB2 amplification in breast cancer analyzed by fluorescence in situ hybridization. Proc Natl Acad Sci U S A *89*, 5321-5325.
Khattri, R., Cox, T., Yasayko, S-A., Ramsdell, F.. (2003). An essential role for scurfin in CD4+CD25+ T regulatory cells. Nat Immunol *4*, 337-342.
Knudson, A.G., Jr. (1971). Mutation and cancer: statistical study of retinoblastoma. Proc Natl Acad Sci U S A *68*, 820-823.
Kristiansen, M., Knudsen, G.P., Maguire, P., Margolin, S., Pedersen, J., Lindblom, A., and Orstavik, K.H. (2005). High incidence of skewed X chromosome inactivation in young patients with familial non-BRCA1/BRCA2 breast cancer. J Med Genet *42*, 877-880.
Love, R.R., Duc, N.B., Allred, D.C., Binh, N.C., Dinh, N.V., Kha, N.N., Thuan, T.V., Mohsin, S.K., Roanh le, D., Khang, H.X., *et al.* (2002). Oophorectomy and tamoxifen

adjuvant therapy in premenopausal Vietnamese and Chinese women with operable breast cancer. J Clin Oncol *20*, 2559-2566.
Love, R.R., Duc, N.B., Havighurst, T.C., Mohsin, S.K., Zhang, Q., DeMets, D.L., and Allred, D.C. (2003). Her-2/neu overexpression and response to oophorectomy plus tamoxifen adjuvant therapy in estrogen receptor-positive premenopausal women with operable breast cancer. J Clin Oncol *21*, 453-457.
Lydon, J.P., Ge, G., Kittrell, F.S., Medina, D., and O'Malley, B.W. (1999). Murine mammary gland carcinogenesis is critically dependent on progesterone receptor function. Cancer Res *59*, 4276-4284.
Miki, Y., Swensen, J., Shattuck-Eidens, D., Futreal, P.A., Harshman, K., Tavtigian, S., Liu, Q., Cochran, C., Bennett, L.M., Ding, W., et al. (1994). A strong candidate for the breast and ovarian cancer susceptibility gene BRCA1. Science *266*, 66-71.
Muller, W.J., Ho, J., and Siegel, P.M. (1998). Oncogenic activation of Neu/ErbB-2 in a transgenic mouse model for breast cancer. Biochem Soc Symp *63*, 149-157.
Nevins, J.R., Leone, G., DeGregori, J., and Jakoi, L. (1997). Role of the Rb/E2F pathway in cell growth control. J Cell Physiol *173*, 233-236.
Onizuka, S., Tawara, I., Shimizu, J., Sakaguchi, S., Fujita, T., and Nakayama, E. (1999). Tumor rejection by in vivo administration of anti-CD25 (interleukin-2 receptor alpha) monoclonal antibody. Cancer Res *59*, 3128-3133.
Piao, Z., and Malkhosyan, S.R. (2002). Frequent loss Xq25 on the inactive X chromosome in primary breast carcinomas is associated with tumor grade and axillary lymph node metastasis. Genes Chromosomes Cancer *33*, 262-269.
Richardson, A.L., Wang, Z.C., De Nicolo, A., Lu, X., Brown, M., Miron, A., Liao, X., Iglehart, J.D., Livingston, D.M., and Ganesan, S. (2006). X chromosomal abnormalities in basal-like human breast cancer. Cancer Cell *9*, 121-132.
Roncuzzi, L., Brognara, I., Cocchi, S., Zoli, W., and Gasperi-Campani, A. (2002). Loss of heterozygosity at pseudoautosomal regions in human breast cancer and association with negative hormonal phenotype. Cancer Genet Cytogenet *135*, 173-176.
Samuels, Y., Wang, Z., Bardelli, A., Silliman, N., Ptak, J., Szabo, S., Yan, H., Gazdar, A., Powell, S.M., Riggins, G.J., *et al.* (2004). High frequency of mutations of the PIK3CA gene in human cancers. Science *304*, 554.
Schechter, A.L., Stern, D.F., Vaidyanathan, L., Decker, S.J., Drebin, J.A., Greene, M.I., and Weinberg, R.A. (1984). The neu oncogene: an erb-B-related gene encoding a 185,000-Mr tumour antigen. Nature *312*, 513-516.
Schmidt, M., Fernandez de Mattos, S., van der Horst, A., Klompmaker, R., Kops, G.J., Lam, E.W., Burgering, B.M., and Medema, R.H. (2002). Cell cycle inhibition by FoxO forkhead transcription factors involves downregulation of cyclin D. Mol Cell Biol *22*, 7842-7852.
Scott, G.K., Chang, C.H., Erny, K.M., Xu, F., Fredericks, W.J., Rauscher, F.J ., Thor, A.D., Benz, C.C.. (2000). Ets regulation of the erbB2 promoter. Oncogene *19*, 6490-6502.
Slamon, D.J., Clark, G.M., Wong, S.G., Levin, W.J., Ullrich, A., and McGuire, W.L. (1987). Human breast cancer: correlation of relapse and survival with amplification of the HER-2/neu oncogene. Science *235*, 177-182.
Slamon, D.J., Leyland-Jones, B., Shak, S., Fuchs, H., Paton, V., Bajamonde, A., Fleming, T., Eiermann, W., Wolter, J., Pegram, M., *et al.* (2001). Use of chemotherapy plus a

monoclonal antibody against HER2 for metastatic breast cancer that overexpresses HER2. N Engl J Med *344*, 783-792.
Spatz, A., Borg, C. and Feunteun, J.. (2004). X-Chromosome genetics and human cancer. Nat Rev Cancer *4*, 617-629.
Struewing, J.P., Hartge, P., Wacholder, S., Baker, S.M., Berlin, M., McAdams, M., Timmerman, M.M., Brody, L.C., and Tucker, M.A. (1997). The risk of cancer associated with specific mutations of BRCA1 and BRCA2 among Ashkenazi Jews. N Engl J Med *336*, 1401-1408.
Sutmuller, R.P., van Duivenvoorde, L.M., van Elsas, A., Schumacher, T.N., Wildenberg, M.E., Allison, J.P., Toes, R.E., Offringa, R., and Melief, C.J. (2001). Synergism of cytotoxic T lymphocyte-associated antigen 4 blockade and depletion of CD25(+) regulatory T cells in antitumor therapy reveals alternative pathways for suppression of autoreactive cytotoxic T lymphocyte responses. J Exp Med *194*, 823-832.
Todorovic-Rakovic, N., Jovanovic, D., Neskovic-Konstantinovic, Z., and Nikolic-Vukosavljevic, D. (2005). Comparison between immunohistochemistry and chromogenic in situ hybridization in assessing HER-2 status in breast cancer. Pathol Int *55*, 318-323.
van de Vijver, M.J., Peterse, J.L., Mooi, W.J., Wisman, P., Lomans, J., Dalesio, O., and Nusse, R. (1988). Neu-protein overexpression in breast cancer. Association with comedo-type ductal carcinoma in situ and limited prognostic value in stage II breast cancer. N Engl J Med *319*, 1239-1245.
Wang, C.Y., Cusack, J.C., Jr., Liu, R., and Baldwin, A.S., Jr. (1999). Control of inducible chemoresistance: enhanced anti-tumor therapy through increased apoptosis by inhibition of NF-kappaB. Nat Med *5*, 412-417.
Weinstein, I.B. (2002). Cancer. Addiction to oncogenes--the Achilles heal of cancer. Science *297*, 63-64.
Wildin, R.S., Ramsdell, F., Peake, J., Faravelli, F., Casanova, J.L., Buist, N., Levy-Lahad, E., Mazzella, M., Goulet, O., Perroni, L., Bricarelli, F.D., et al.. (2001). X-linked neonatal diabetes mellitus, enteropathy and endocrinopathy syndrome is the human equivalent of mouse scurfy. Nat Genet *27*, 18-20.
Wooster, R., Bignell, G., Lancaster, J., Swift, S., Seal, S., Mangion, J., Collins, N., Gregory, S., Gumbs, C., Micklem, G.. (1995). Identification of the breast cancer susceptibility gene BRCA2. Nature *378*, 789-792.
Wooster, R.a.W., B.L. (2003). Breast and Ovarian Cancer. The New England Journal of Medicine *348*, 2339-2347.
Xing, X., Wang, S.C., Xia, W., Zou, Y., Shao, R., Kwong, K.Y., Yu, Z., Zhang, S., Miller, S., Huang, L., Hung, M.C.. (2000). The ets protein PEA3 suppresses HER-2/neu overexpression and inhibits tumorigenesis. Nat Med *6*, 189-195.
Yaziji, H., Goldstein, L.C., Barry, T.S., Werling, R., Hwang, H., Ellis, G.K., Gralow, J.R., Livingston, R.B., and Gown, A.M. (2004). HER-2 testing in breast cancer using parallel tissue-based methods. JAMA *291*, 1972-1977.
Yu, Y., Okayasu, R., Weil, M.M., Silver, A., McCarthy, M., Zabriskie, R., Long, S., Cox, R., and Ullrich, R.L. (2001). Elevated breast cancer risk in irradiated BALB/c mice associates with unique functional polymorphism of the Prkdc (DNA-dependent protein kinase catalytic subunit) gene. Cancer Res *61*, 1820-1824.
Ziegler, S.F. (2005). FOXP3: Of Mice and Men. Annu Rev Immunol.

Figure legends

Fig. 1. Increased susceptibility to breast cancer in mice heterozygous for *Foxp3*^{sf}. **A.** Representative breast cancers developed in female *Foxp3*$^{sf/+}$*Otc*$^{spf/+}$ mice. The top panel shows the gross anatomy while the lower panel shows the histology of local and metastatic lesions of a breast cancer. **B.** Cancer-free survival analysis of *Foxp3*$^{sf/+}$, *Foxp3*$^{sf/+}$*Otc*$^{spf/+}$, *Otc*$^{spf/+}$ and WT littermates. Mice were sacrificed when moribund to identify the tissue origins of cancers. *Foxp3*$^{sf/+}$ vs. WT, P<0.0001; *Foxp3*$^{sf/+}$ vs. *Otc*$^{spf/+}$, P=0.0003; *Foxp3*$^{sf/+}$ vs. *Foxp3*$^{sf/+}$*Otc*$^{spf/+}$, P=0 .9526; *Foxp3*$^{sf/+}$*Otc*$^{spf/+}$ vs. WT, P=0.0001; *Foxp3*$^{sf/+}$*Otc*$^{spf/+}$ vs. Otc$^{spf/+}$, P=0.0001; *Otc*$^{spf/+}$ vs. WT, P=0.4164. **C.** As in B, except that only incidences of mammary tumors were included. *Foxp3*$^{sf/+}$ vs. Wt: P=0.00015, *Foxp3*$^{sf/+}$*Otc*$^{spf/+}$ vs. WT: P=0.00011. **D**. Increased susceptibility of *Foxp3*$^{sf/+}$ mice to carcinogen DMBA and progesterone. The diagram on top depicts experimental protocol, while survival analysis is shown in the bottom panel. *Foxp3*$^{sf/+}$ vs. WT, P<0.0001; *Foxp3*$^{sf/+}$*Otc*$^{spf/+}$ vs. Otc$^{spf/+}$, P=0.0005; *Otc*$^{spf/+}$ vs. WT, P=0.8157. In B & C, those mice that were observed for only part of the duration were incorporated as censored samples and were marked with a cross in the Kaplan-Meier survival curves. P values in B&C were derived from log-rank test.

Fig. 2. Inactivation of the WT *Foxp3* allele in mammary cancer cells. **A.** Defective *Foxp3* expression in breast cancer. Total RNA extracted from the cells procured by LCM was subjected to quantitative real-time RT-PCR using primers

specific for *Foxp3, Hprt* and *CK19*. In the left panel, fluorescence intensity (∆Rn) was plotted versus cycle number. Mean and S.D. from three individual mice per group are presented in the right panel (P<0.0001, one-way ANOVA test when either internal standard was used)**. B.** Immunohistochemical staining of normal mammary glands and adenocarcinomas from a *Foxp3*$^{sf/+}$*Otc*$^{spf/+}$ mouse using rabbit anti-FOXP3 polyclonal antibody and normal rabbit IgG as the control. **C.** Specific silencing of the WT allele in breast cancer cells. *Foxp3* transcripts were amplified from micro-dissected breast cancers or normal breast epithelium by two rounds of anchored PCR and were cloned into the TOPO vector and sequenced. Left panels show the chromatograms of the mutant (top) and WT transcripts. The right panel shows the number of clones with sequences of WT or mutant alleles in the breast cancer and normal epithelium. A total of 20 clones were sequenced from each group. Data shown are from pooled samples that lack *CD3* transcripts. n.d., not detectable.

Fig 3. *Foxp3* represses the expression of *ErbB2.* **A**. Over-expression of *ErbB2* in mouse mammary cancers. Top panels show immunohistochemical staining of a non-cancerous mammary gland and an adjacent adenocarcinoma from a *Foxp3*$^{sf/+}$*Otc*$^{spf/+}$ mouse using anti-ErbB2 antibody. Lower panel: Relative expression levels of *ErbB2* in normal mammary epithelium of *WT* and *Foxp3*$^{sf/+}$*Otc*$^{spf/+}$ mice and of cancer tissues from *Foxp3*$^{sf/+}$*Otc*$^{spf/+}$ mice as revealed by real-time RT-PCR of LCM samples. Data shown are means and S.D. The expression of *ErbB2* was normalized against either *Hprt* or *CK19*. Highly

significant differences were observed between cancerous and normal tissue (P<0.001, ANOVA test when either internal standards were used). **B.** Transfection of *Foxp3-V5* into TSA cells repressed expression of the *ErbB2* locus. The left panel shows mRNA levels as measured by real-time PCR. Data shown are means and S.D. of triplicates. The right panel shows the protein levels by Western blot of the cell lysates using anti-ErbB2 antibody. The amount of actin β was used as loading control, while the amount of transfected Foxp3-V5 was measured by Western blot using anti-V5 antibodies. **C.** Binding of the Foxp3-V5 fusion protein to the promoter region of the *ErbB2* gene. Top panel is a diagram of the 5' region of the *ErbB2* gene, including the promoter, exon 1, intron 1 and exon 3. The forkhead binding motifs are illustrated with small green bars, while the regions surveyed by real-time PCR are marked in red bars. The lower panel shows the amount of DNA precipitated by either control IgG or anti-V5 mAb expressed as % of the total input genomic DNA. **D.** *Foxp3*-mediated repression of the *ErbB2* promotor requires forkhead binding motifs as evaluated by dual-luciferase^R reporter assay. The promoter regions differed in the number of forkhead binding motifs, as illustrated in the diagram in the left. Three different cell lines were transfected with either vector control or *Foxp3* (1 μg/well) in conjunction with the luciferase reporter driven by different 5' promoter regions of the *ErbB2* gene (0.6 μg/well). pRL-TK was used as internal control. The luciferase activity from the cells transfected with the pGL2-basic vector was arbitrarily defined as 1.0. Data shown are means and S.D. of triplicates and have been repeated at least three times. Real-time PCR indicated that the level of

Foxp3 transcripts in the transfected cell line was about 6-fold of what was found in the micro-dissected mammary epithelial cells. However, this is likely an over-estimate, as the expression of *Foxp3* is likely heterogenous among the ex vivo epithelial cells (data not shown) and as the recovery for the labile RNA from the ex vivo cells is less efficient than the stable cell lines. **E.** Site-directed mutagenesis of one of two conserved regions with multiple forkhead binding motifs in the *ErbB2/HER-2* promoters prevented repression of *ErbB2* promoter by *Foxp3*. Left panel is a diagram of human *HER-2* and mouse *ErbB2* promoters. The homologous region between the two promoters are indicated by arrows, and the two binding sites were deleted individually (deleted DNA sequence, mut A: AAATCTGGGATCATTTA; Mut B: TTTGAATTTCAGATAAA). Right panel shows that mutations of either site prevented *FOXP3*-mediated suppression. The promoter activity was measured and normalized as detailed in D, except that the amount of promoter DNA was 0.4 μg/sample. The promoter activities of the vector groups were artificially defined as 1.0. **F.** Foxp3 mediated binding to specific cis-elements in the *ErbB2* promoter. Nuclear extracts from the F*oxp3-V5*- (F-NE) or vector-transfected control (C-NE) TSA cells were pre-incubated with ^{32}P-labeled WT (*W) or mutant probes (*M) in the presence of an unlabeled WT (W) or mutant probe (M) . The mixtures were analyzed by PAGE. NS, nonspecific; FP, free probe. The specific Foxp3-shifted band is marked by an arrow. Data shown have been repeated three times. **G**. Mutation of forkhead binding motifs (mut C) abrogated FOXP3-mediated repression, but not basal promoter activity. As in **E,** except that WT, mut B and mut C (mutations that

inactivate the Foxp3 binding as detailed in F) of the *ErbB2* promoters were used. This experiment has been repeated twice with similar results. The differences were compared by student t-tests with P value provided.

Fig. 4. Characterization of *FOXP3* transcripts in primary, immortalized and malignant mammary epithelial cells. **A.** Relative levels and isoforms of *FOXP3* and *HER-2* mRNA. After normalizing against endogenous *GAPDH*, the amounts of transcripts were compared to those found in HMEC-1, which was arbitrally defined as 1.0. The reported ER status and the isoforms of the *FOXP3* transcripts detected are indicated. To characterize the isoforms, *FOXP3* mRNA was amplified by two rounds of anchored PCR using primers annealing to exons 1 and 12. The bulk PCR products were sequenced only if one species was found in agarose electrophoresis. When more than one species was observed, the PCR products were cloned and multiple clones were sequenced until all of the species observed in the agarose gel were identified. **B.** Sequencing profiles of alternatively spliced *FOXP3* mRNA lacking exons 3 & 4, which resulted in a frame-shift and early termination codon. The profile of a full length *FOXP3* mRNA is shown for comparison.

Fig. 5. *FOXP3* defects in human breast cancer. **A**. Down-regulation of the FOXP3 protein among human breast cancer cells. Photographs in the top and middle panels show immunohistochemical staining of normal and carcinoma tissues from the same patient. The number and percentage of FOXP3 positive

tissues are shown in the lower panel. Samples with nuclear staining by the anti-Foxp3 antibody were scored as positive. **B**. Deletion of the *FOXP3* locus in breast cancer cells. Breast cancer tissue microarray samples were analyzed by FISH using 3 BAC clone probes surrounding a 10MB region in Xp11.2. A typical FISH for the CEPX (green) and *FOXP3* (orange) probes is shown on the left, while the genomic structure of the X-chromosome and probe positions are illustrated in the middle panel. A total of 238 samples were analyzed for all probes, with 223 samples providing definitive FISH data. 28/223 samples showed deletions as detected by at least one of the 3 probes. The positions of the deletions in the 28 samples are summarized in the right panel. **C&D**. Somatic mutation of the *FOXP3* gene in breast cancer samples. Genomic DNA was isolated from matched normal and cancerous tissues from 65 breast cancer patients and amplified with primers for individual exons and intron-exon boundary regions. Somatic mutations were identified by comparing sequences from normal and cancerous samples from the same patients. The data are from either bulk sequencing of PCR products or from the sequencing of 5-10 clones from PCR products. Only those mutations that were observed in multiple clones were scored. **C.** A representative chromatogram of DNA sequencing, with a mutation in codon 88 from glycine to aspartic acid and a loss of the WT allele. **D.** Summary of all mutations found in 65 cases. Note that some publications do not include the non-coding exon 1, therefore differing in exon numbering by 1. Mutations identified from 50 cases of formalin fixed samples are marked in black, while those identified from 15 cases of frozen tissue samples are marked in red.

E. *FOXP3* mutations reduced its repressor activity for the *HER-2* promoter in the SKBr-3 cell line. Top panel shows expression of mutant cDNA. The middle panel shows luciferase activity, while the lower panel shows the levels of *HER-2* transcripts. For luciferase assay, the 2.1kb *HER-2* promoter linked to the luciferase reporter (0.25 μg/well) was co-transfected with 1 μg/well of either vector control, WT or two mutants of the FOXP3 isolated from breast cancer tissues (338 P>L in the FKH domain or 204C>R/205E>K in the zinc finger domain). The luciferase activity was measured at 48 hours after transfection. For the expression of *HER-2* by real-time PCR, the transfectant were selected with blasticidin for one week and RNA was isolated from drug resistant cells and used to prepare cDNA. In both readouts, the difference between WT and 318 P> L and that between WT and 204C>R205E>K are highly significant ($P<0.01$). Data shown are representative of at least 2-3 independent experiments. **F**. A breast cancer sample with a somatic mutation in intron 6 (case 23) had an inactivated *FOXP3* locus. Normal mammary epithelial (N) and tumor (T) cells were isolated by laser-guided micro-dissection. The *FOXP3* transcripts were determined either by PCR using primers spanning exons 5-8 to detect alternatively spliced products or by real-time PCR using primers spanning exons 10-12. The upper and middle panels show photographs of PCR products of *FOXP3* or *GAPDH* loci, while the lower panel shows the relative level of *FOXP3* transcripts as determined by real time PCR. Neither assay detected any *FOXP3* transcripts in the tumor of case No. 23. Substantial amounts of *FOXP3*

transcripts were detected in normal samples and tumors in case 22 (with a synonymous mutation in exon 7), which was artificially defined as 1.0.

Fig. 6. *FOXP3* is an important *HER-2* repressor. **A.** Silencing of FOXP3 resulted in the up-regulation of HER-2 in primary human mammary epithelial cells (HMEC). HMEC were transduced with lentiviral vector for either control sequence or *FOXP3* siRNA. The untransfected cells were removed by selection with blasticidin. At one week after transduction, the levels of the *FOXP3* and *HER-2* transcripts were quantitated by real-time PCR. Data shown are mean and SEM of relative levels of transcripts (with that in the vector-transduced cells defined as 1.0) and represent those of three independent experiments. **B.** Flow cytometry data showing the effect of FOXP3 silencing on HMEC surface HER-2 levels. HER-2-negative MDA-MB468, HER-2^{lo} MCF-7 and HER-2^{hi} SKBr3 cell lines were included for comparison. **C**. In the Tet-off inducible *FOXP3*-expressing BT474, *FOXP3* repressed *HER-2*. BT474 cells were first transfected with pTet-Off vector. The transfectants were selected by both blasticidin and G418 in doxycycline-containing medium. The drug-resistant cells were cultured in the absence of doxycycline for 5 days to induce FOXP3. The cells were stained for FOXP3 and HER-2 proteins by flow cytometry. Data shown are histograms depicting HER-2 levels among the gated FOXP3^{hi} and FOXP3^{-} cells based on reactivity to the anti-Foxp3 antibody and are representative of those from two independent experiments. **D.** Inverse correlation between FOXP3 expression and the HER-2 score among the human breast cancer samples. Tissue microassay

samples were stained with either anti-FOXP3 antibodies or anti-HER-2 antibodies and were scored by two different pathologists in a double blind fashion. FOXP3 staining was scored by positivity of nuclear staining with affinity-purified anti-FOXP3 antibodies. The P values of the chi-square tests are listed. **E.** Inverse correlations between FOXP3 expression and HER-2 scores in cells with or without *HER-2* amplification. The *HER-2* gene copy number was determined by FISH, while nuclear expression of FOXP3 was determined by immunohistochemistry. Data shown are mean and S.D. of HER-2 scores of 425 cases of breast cancers grouped by *HER-2* copy number. P values were generated by the Mann-Whitney test.

Fig. 7. *Foxp3* inhibits the growth and tumorigenicity of multiple breast cancer cell lines. **A**. Breast cancer cell lines MCF-7, SKBr3 and TSA were transfected with equal concentrations of either vector alone (Vector), *Foxp3* or *Otc* cDNA. After 3 weeks of G-418 selection, the drug resistant clones were visualized by crystal violet dye. **B**. Summary of the colony numbers in three independent experiments as described in A. Data shown are means and S.D. **C.** Somatic mutations identified from breast cancer samples attenuated the growth suppression of the FOXP3. As in A & B, except that two somatic mutants were compared with WT *FOXP3* cDNA using the two human breast cancer cell lines. Expression of WT and mutant proteins at 1 week after transfection is presented in the insert. **D&E**. Ectopic expression of the *ErbB2* but not the *c-Myc* cDNA abrogated *Foxp3*-mediated repression. TSA cells were transfected with either pcDNA6-blasticidin

vector or *ErbB2* cDNA and selected with blasticidin for two weeks. Pools of blasticidin-resistant cells were super-transfected with the pEF1-G418 vector or *Foxp3* cDNA. The cells were then plated and selected with blasticidin and G418 for three weeks. The viable colonies were visualized after staining with the crystal violet dye. **D**. Photographs of a representative plate showing abrogation of *Foxp3*-mediated suppression by *ErbB2*. **E**. The mean and S.D. of the colony numbers. This experiment has been repeated twice with essentially identical results. **F**. Expression of *Foxp3* reduced growth rate of tumors. Syngeneic BALB/c mice were injected with $5x10^5$/mouse *Foxp3* or vector-transfected TSA cells in the flank and the sizes of the local tumor mass were measured using a caliper. Data shown are means and S.D. and have been repeated once. **G**. The survival of tumor-bearing mice was monitored over a 7-weeks period. As in F, except that 10^6 tumor cells /mouse were injected and the mice were euthanized when they became moribund. A significant difference was observed in the survival of mice bearing the different types of tumor cells (P=0.0015, log-rank test).

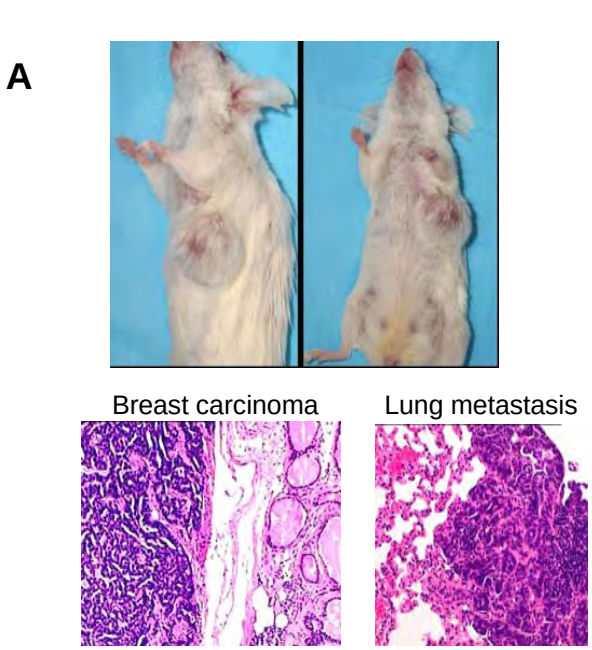
A
Breast carcinoma
Lung metastasis
B
Spontaneous tumors
Tumor-free survival
Months
Otc spf/+ (n=16)
WT (n=35)
Otc spf/+ Foxp3 sf/+ (n=55)
Foxp3 sf/+ (n=18)
C
Incidence of mammary tumor
Tumor- free Survival
Months
Otc spf/+ (n=16)
WT (n=35)
Otc spf/+ Foxp3 sf/+ (n=55)
Foxp3 sf/+ (n=18)
D
Medroxyprogesterone 50mg
DMBA 1mg/dose
Age (Weeks)
Tumor-free survival
Time after treatment (Weeks)
Otc spf/+ (n=20)
WT (n=26)
Foxp3 sf/+ (n=34)

Fig. 1

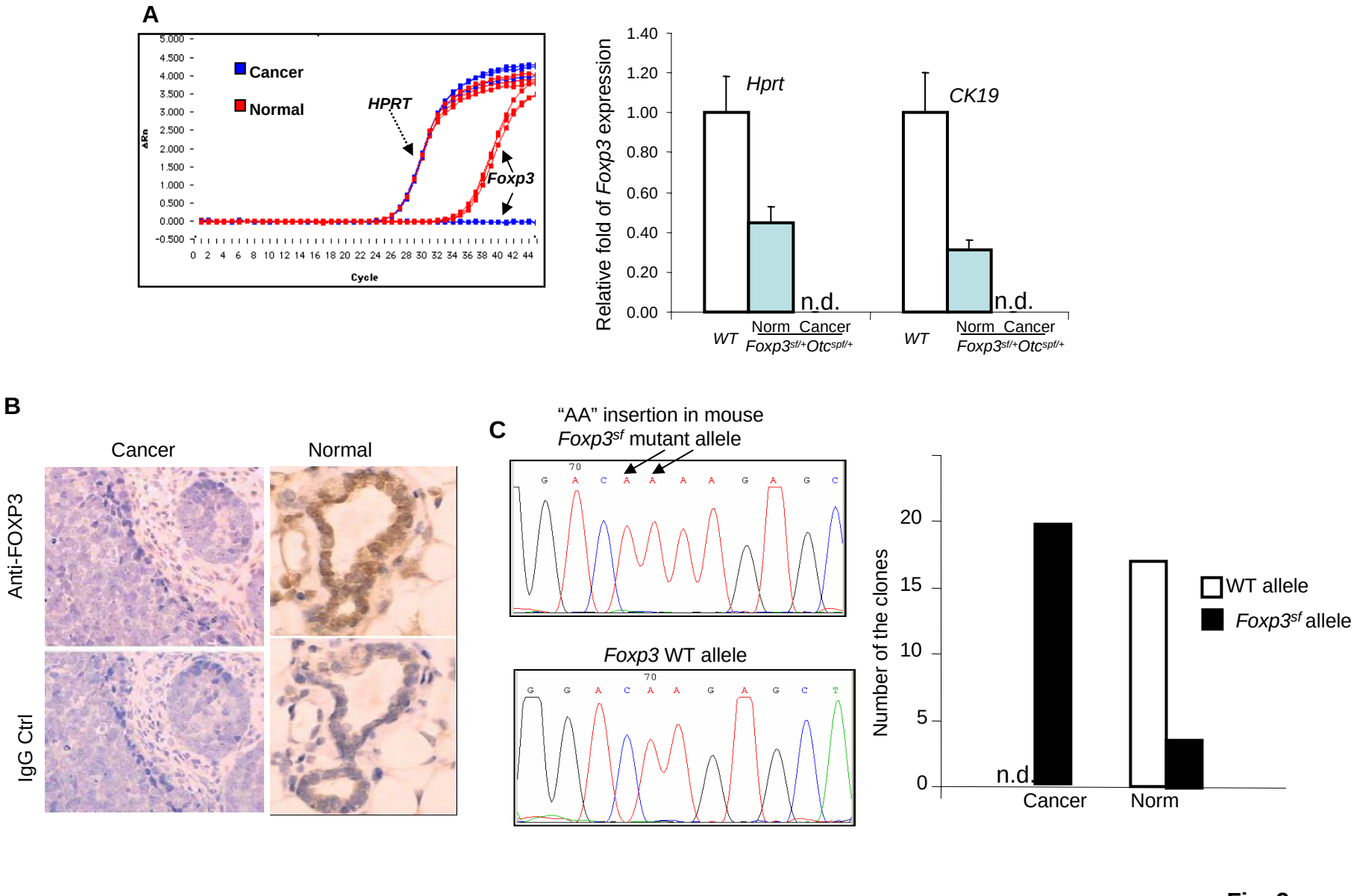
A
Cancer
Normal
HPRT
Foxp3
ΔRn
Cycle
Relative fold of Foxp3 expression
Hprt
CK19
n.d.
n.d.
WT
Norm Cancer
Foxp3sf/+Otcspf/+
B
Cancer
Normal
Anti-FOXP3
IgG Ctrl
C
"AA" insertion in mouse
Foxp3sf mutant allele
Foxp3 WT allele
Number of the clones
WT allele
Foxp3sf allele
n.d.
Cancer
Norm

Fig. 2

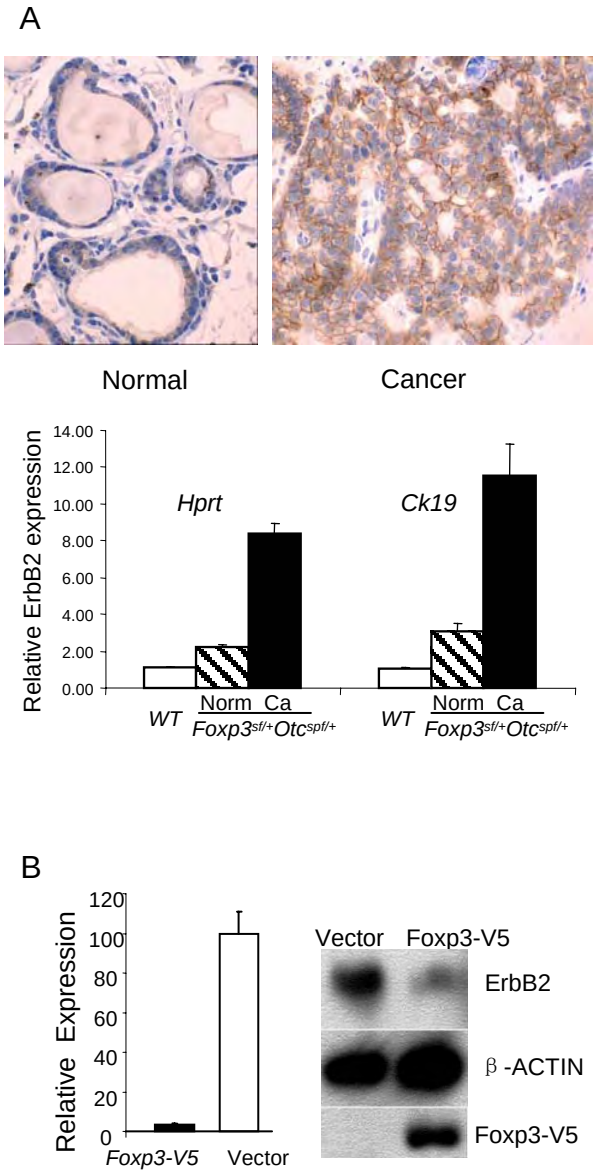
A
Normal
Cancer
Relative ErbB2 expression
14.00
12.00
10.00
8.00
6.00
4.00
2.00
0.00
Hprt
Ck19
WT
Norm Ca
Foxp3sf/+Otcspf/+
WT
Norm Ca
Foxp3sf/+Otcspf/+
B
Relative Expression
120
100
80
60
40
20
0
Foxp3-V5
Vector
Vector
Foxp3-V5
ErbB2
β -ACTIN
Foxp3-V5

Fig. 3-1.

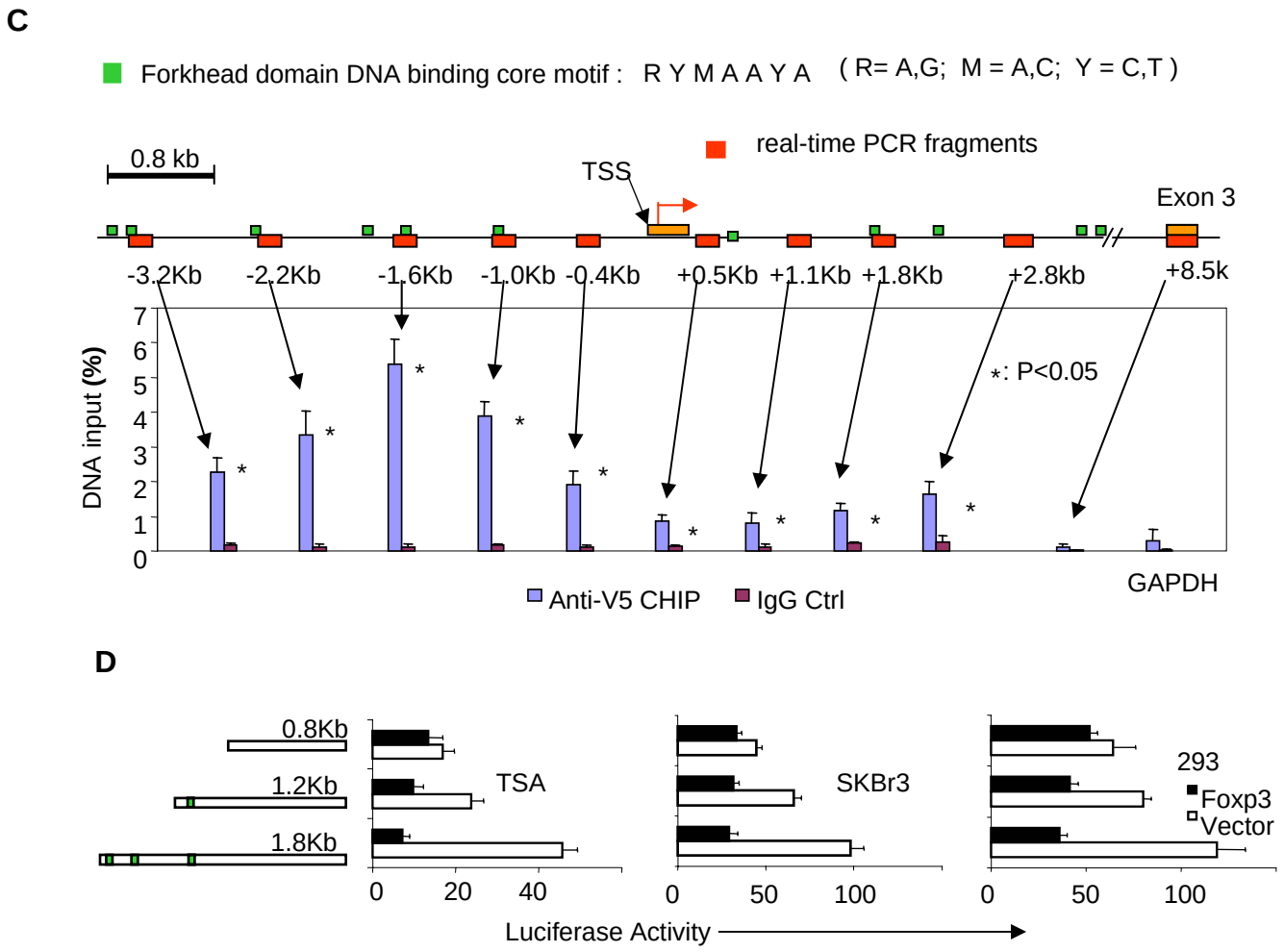
C
Forkhead domain DNA binding core motif : R Y M A A Y A (R= A,G; M = A,C; Y = C,T)
real-time PCR fragments
0.8 kb
TSS
Exon 3
-3.2Kb
-2.2Kb
-1.6Kb
-1.0Kb
-0.4Kb
+0.5Kb
+1.1Kb
+1.8Kb
+2.8kb
+8.5k
DNA input (%)
*: P<0.05
GAPDH
Anti-V5 CHIP
IgG Ctrl
D
0.8Kb
1.2Kb
1.8Kb
TSA
SKBr3
293
Foxp3
Vector
Luciferase Activity

Fig. 3-2

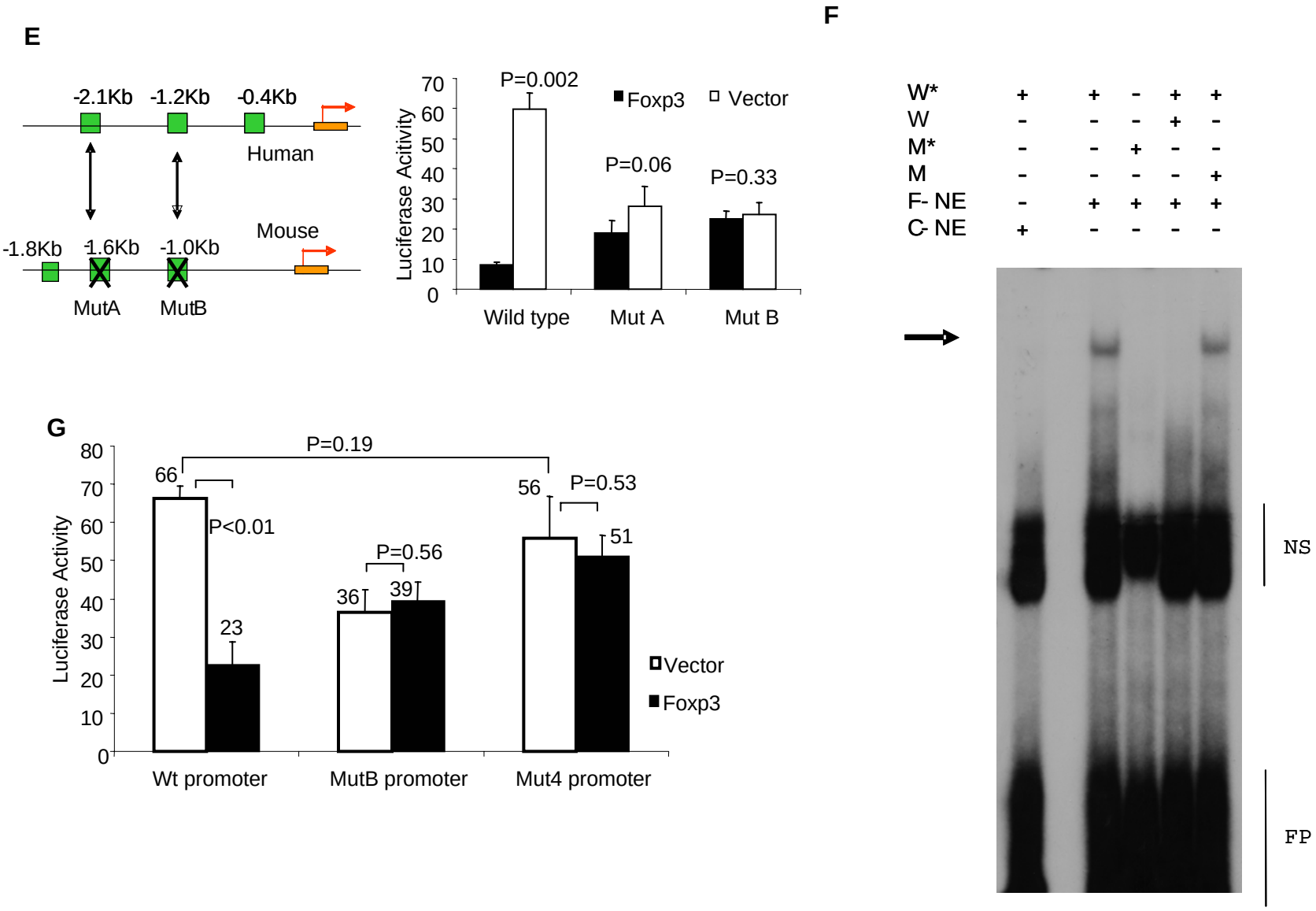
E
-2.1Kb
-1.2Kb
-0.4Kb
Human
-1.8Kb
-1.6Kb
-1.0Kb
Mouse
MutA
MutB
Luciferase Acitivity
P=0.002
P=0.06
P=0.33
Foxp3
Vector
Wild type
Mut A
Mut B
F
W*
W
M*
M
F- NE
C- NE
NS
FP
G
Luciferase Activity
P=0.19
66
P<0.01
23
P=0.56
36
39
56
P=0.53
51
Vector
Foxp3
Wt promoter
MutB promoter
Mut4 promoter

Fig. 3-3

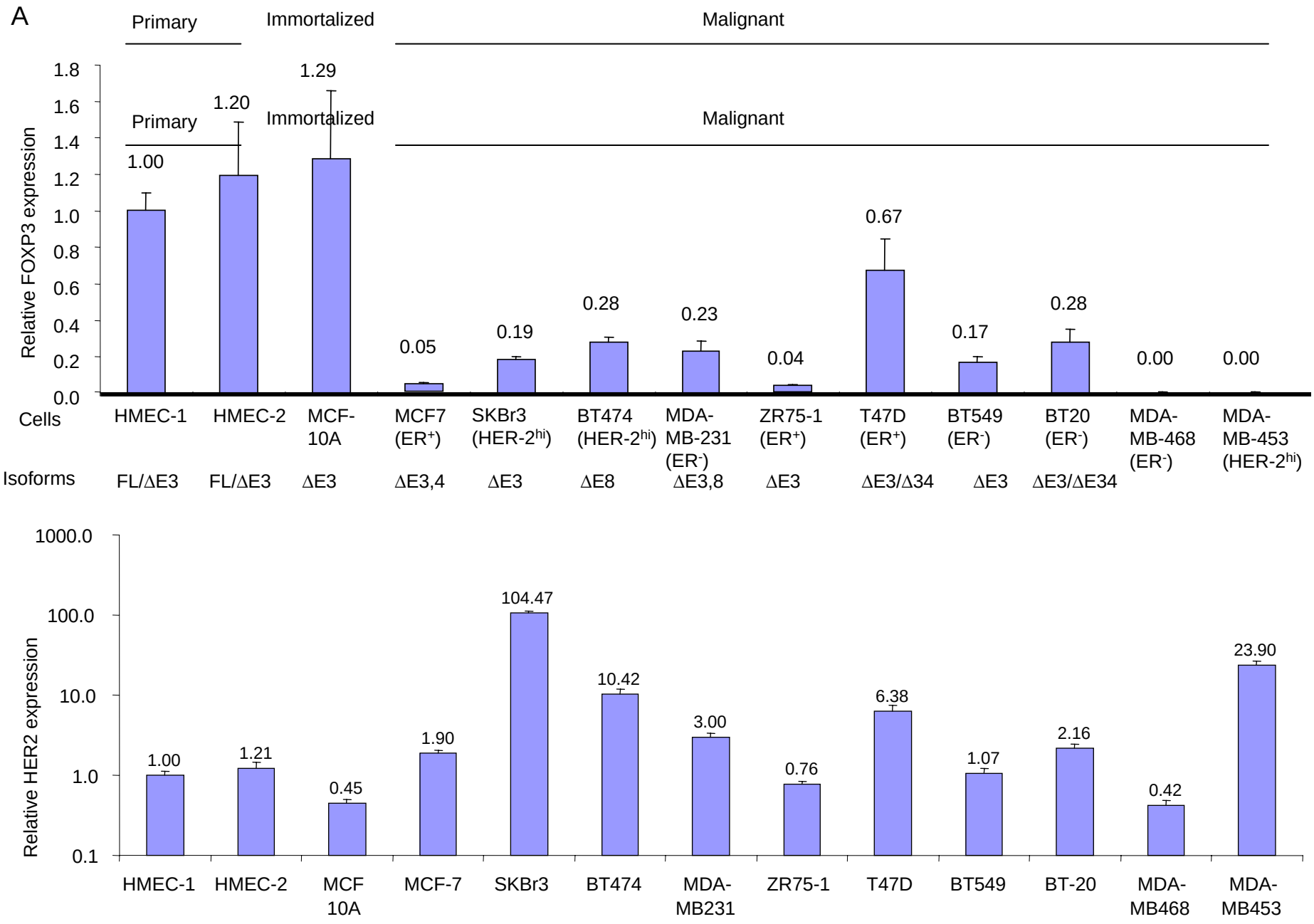
A
Primary
Immortalized
Malignant
Relative FOXP3 expression
1.8
1.6
1.4
1.2
1.0
0.8
0.6
0.4
0.2
0.0
1.00
1.20
1.29
0.05
0.19
0.28
0.23
0.04
0.67
0.17
0.28
0.00
0.00
Cells
HMEC-1
HMEC-2
MCF-10A
MCF7 (ER+)
SKBr3 (HER-2hi)
BT474 (HER-2hi)
MDA-MB-231 (ER-)
ZR75-1 (ER+)
T47D (ER+)
BT549 (ER-)
BT20 (ER-)
MDA-MB-468 (ER-)
MDA-MB-453 (HER-2hi)
Isoforms
FL/ΔE3
FL/ΔE3
ΔE3
ΔE3,4
ΔE3
ΔE8
ΔE3,8
ΔE3
ΔE3/Δ34
ΔE3
ΔE3/ΔE34
Relative HER2 expression
1000.0
100.0
10.0
1.0
0.1
1.00
1.21
0.45
1.90
104.47
10.42
3.00
0.76
6.38
1.07
2.16
0.42
23.90
HMEC-1
HMEC-2
MCF 10A
MCF-7
SKBr3
BT474
MDA-MB231
ZR75-1
T47D
BT549
BT-20
MDA-MB468
MDA-MB453

Fig. 4-1

B

Full length

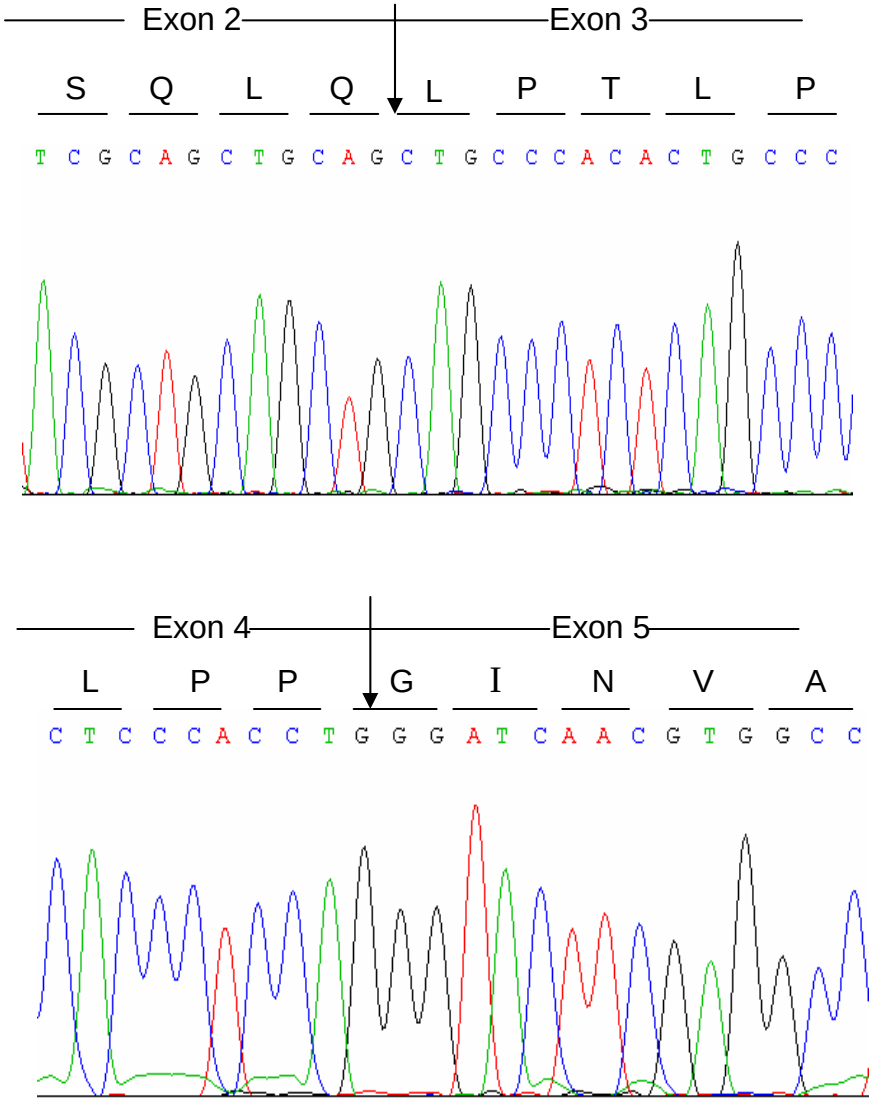

MCF-7

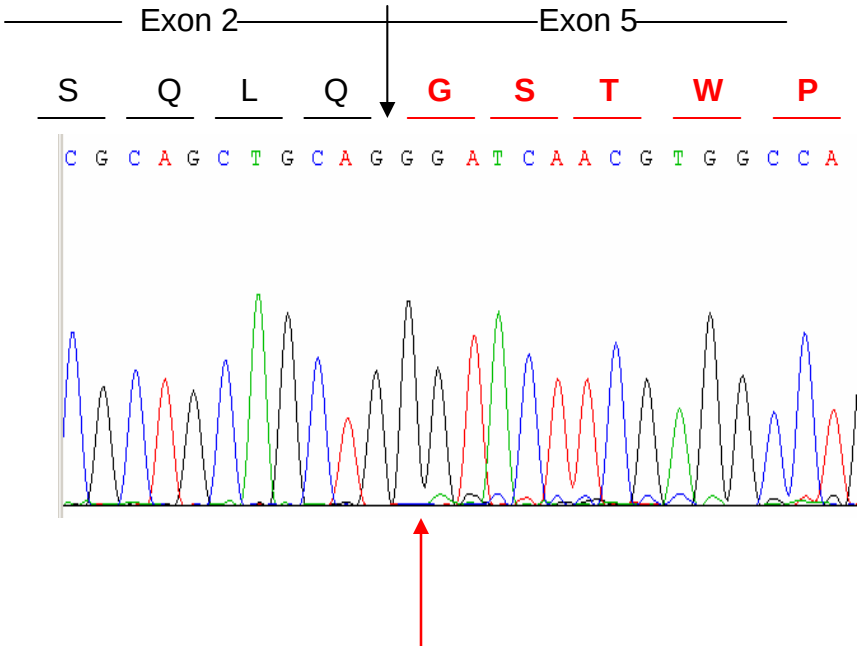

Frame-shift causing early termination at codon172

Fig. 4-2

A

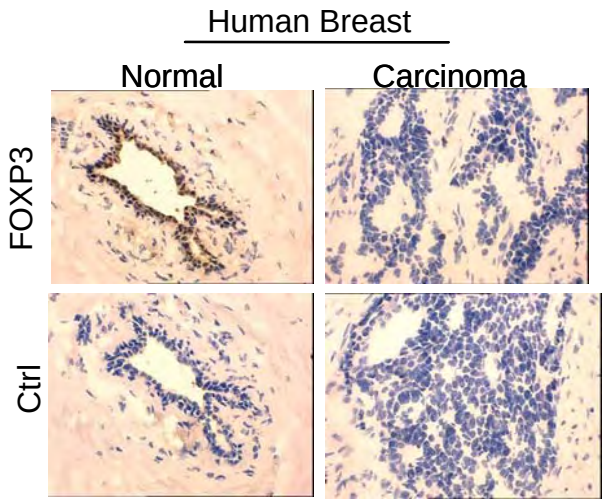

	FOXP3(+)	*FOXP3*(-)	P (vs. normal)
Normal	39	11	
Cancer	58	217	6.0×10^{16}
ER+	30	65	1.0×10^{7}
ER-	28	152	8.2×10^{18}

Fig. 5-1

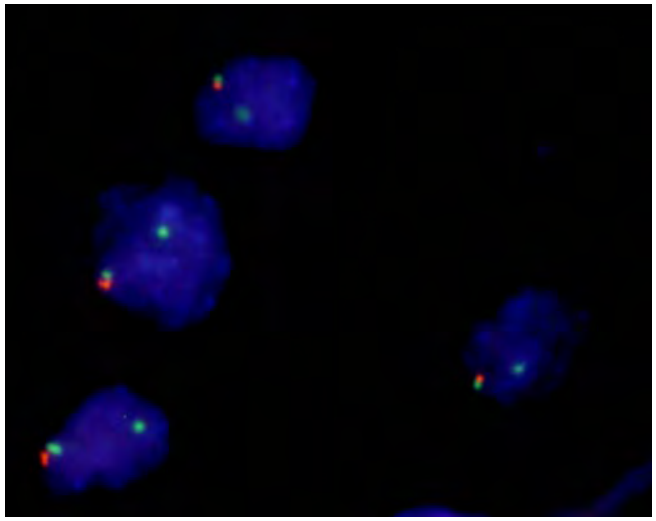

CEPX RP11-344O14 (*FOXP3*)

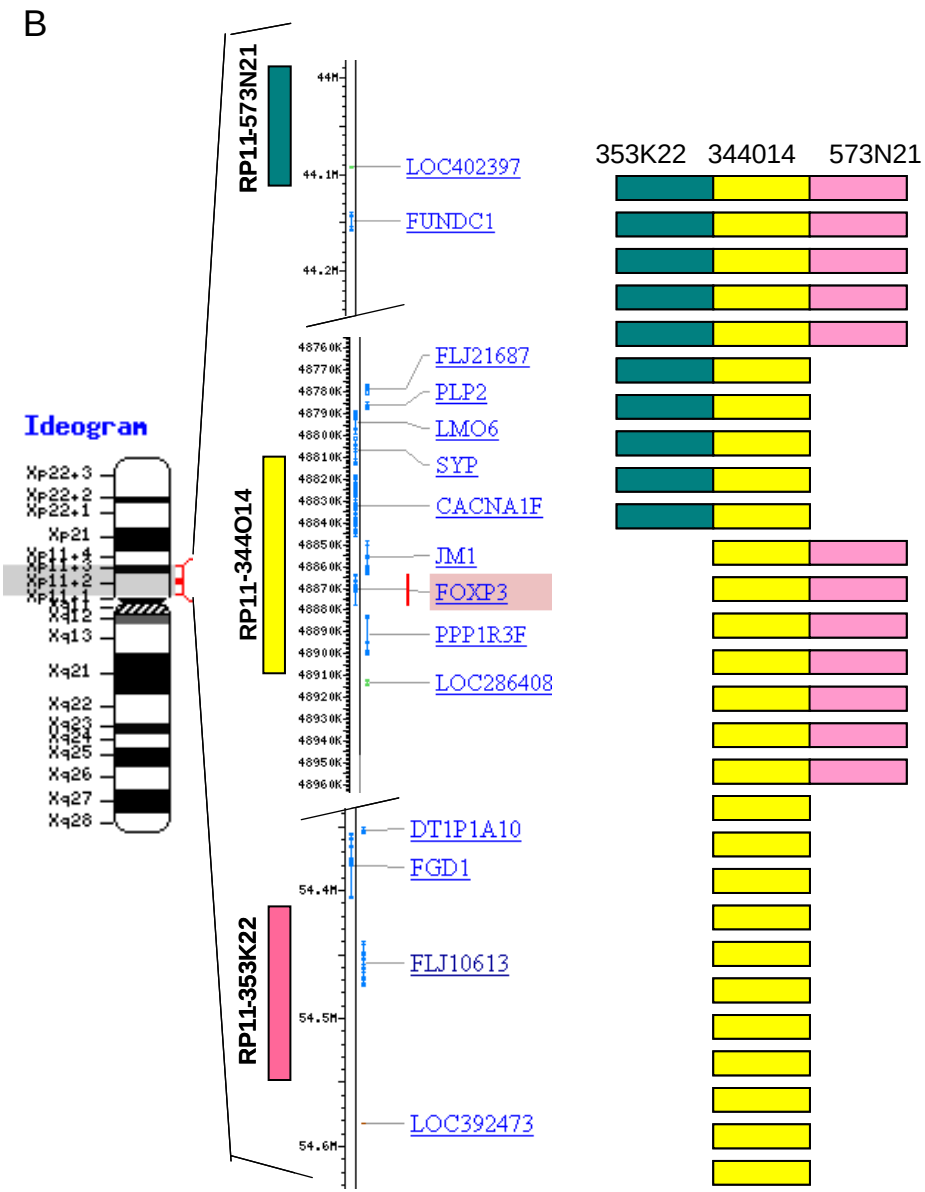

Fig. 5-2

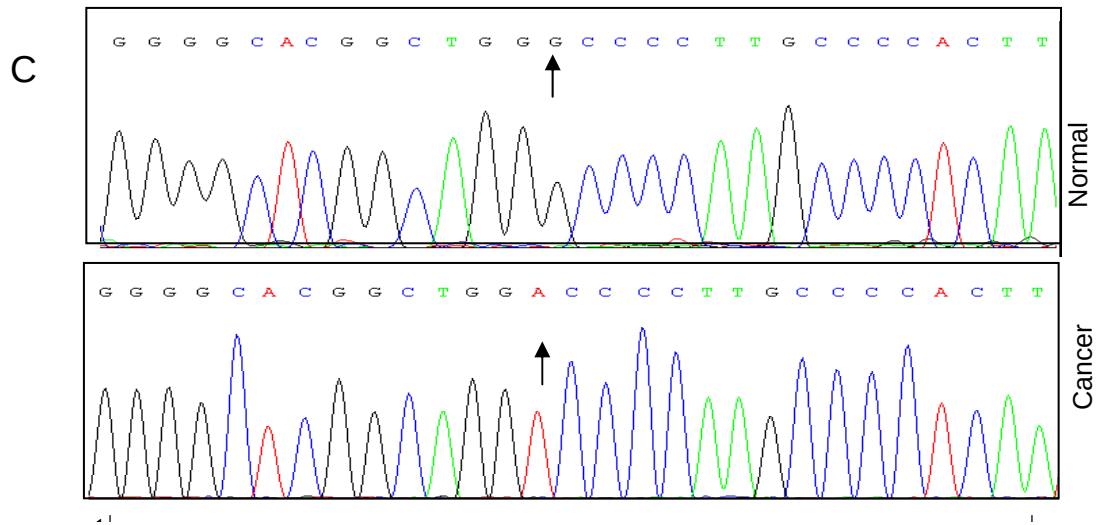
C
Normal
Cancer

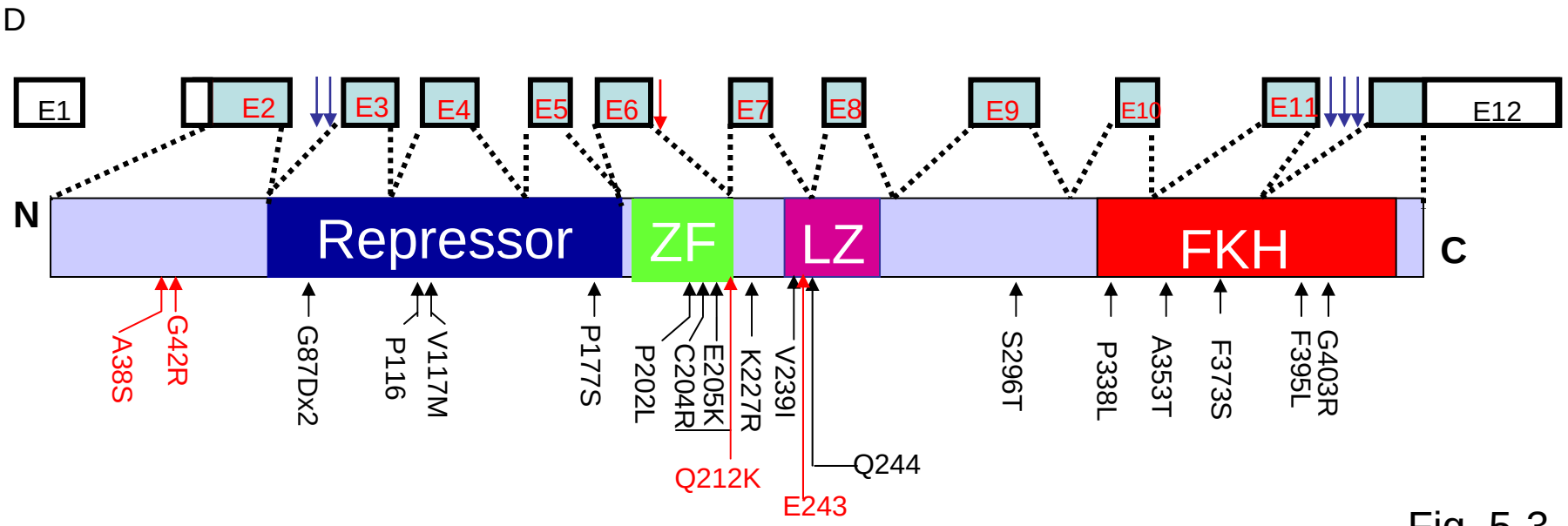
D
E1
E2
E3
E4
E5
E6
E7
E8
E9
E10
E11
E12
N
Repressor
ZF
LZ
FKH
C
A38S
G42R
G87Dx2
P116
V117M
P177S
P202L
C204R
E205K
Q212K
K227R
E243
V239I
Q244
S296T
P338L
A353T
F373S
F395L
G403R

Fig. 5-3

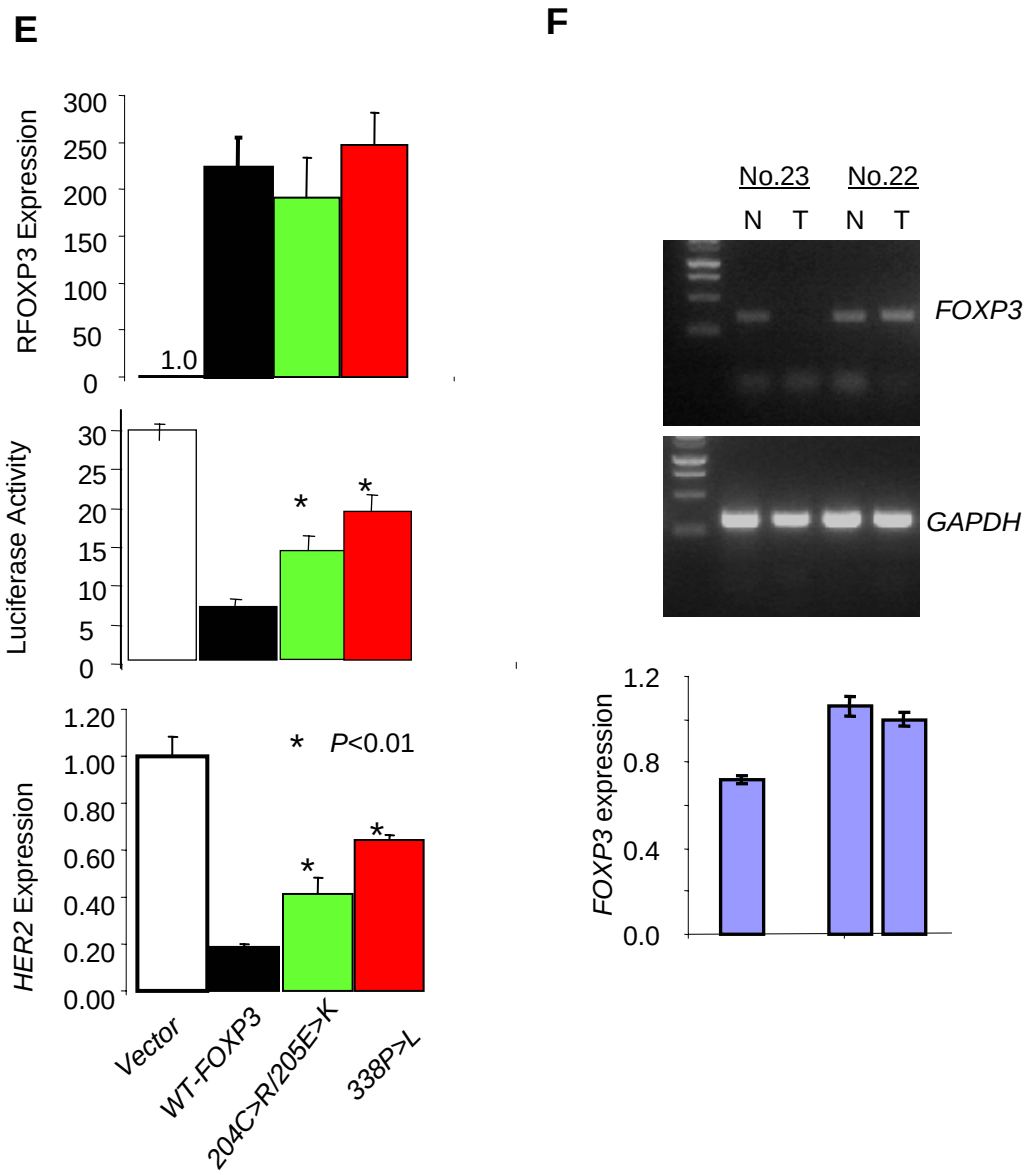
E
RFOXP3 Expression
300
250
200
150
100
50
0
1.0
Luciferase Activity
30
25
20
15
10
5
0
*
*
HER2 Expression
1.20
1.00
0.80
0.60
0.40
0.20
0.00
* P<0.01
*
*
Vector
WT-FOXP3
204C>R/205E>K
338P>L
F
No.23
No.22
N T N T
FOXP3
GAPDH
FOXP3 expression
1.2
0.8
0.4
0.0

Fig. 5-4

A

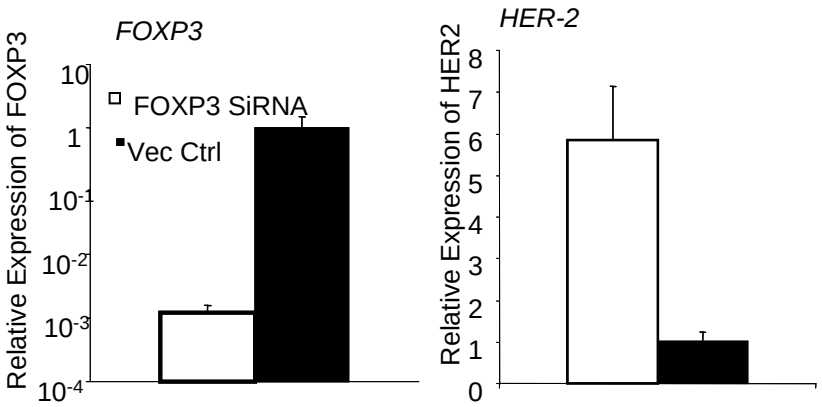

B

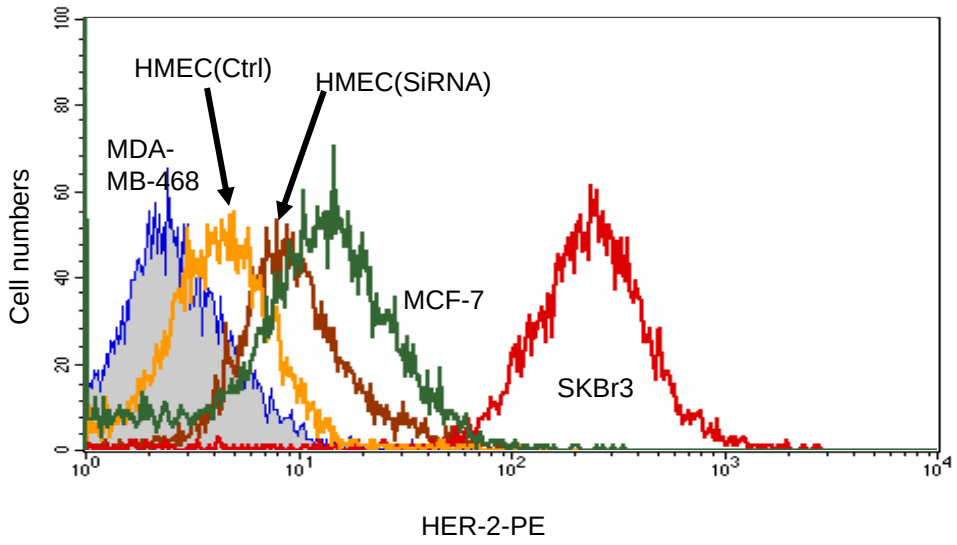

C

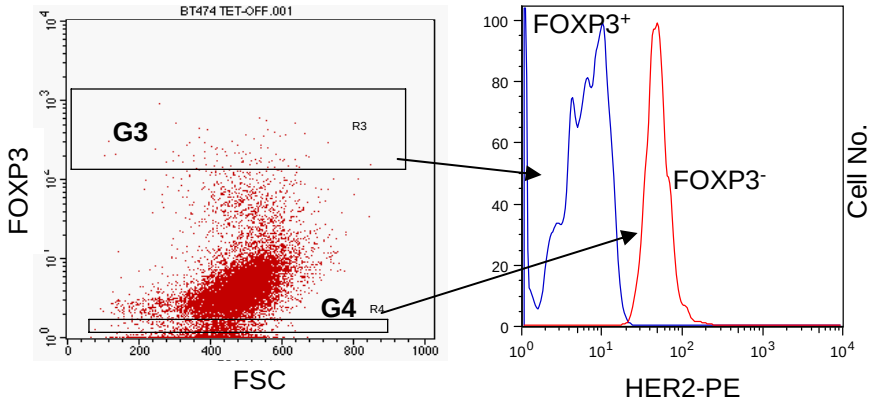

D

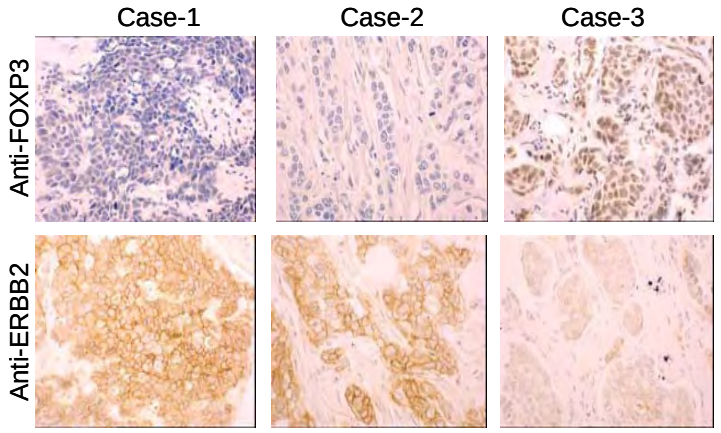

	FOXP3(-)	*FOXP3* (+)	P
Her2 (-)	277	118	
Her2 (+)	87	18	
Her2 (++)	71	6	
Her2 (+++)	82	3	
Total	517	145	1.5×10^{-8}

Fig. 6-1

E

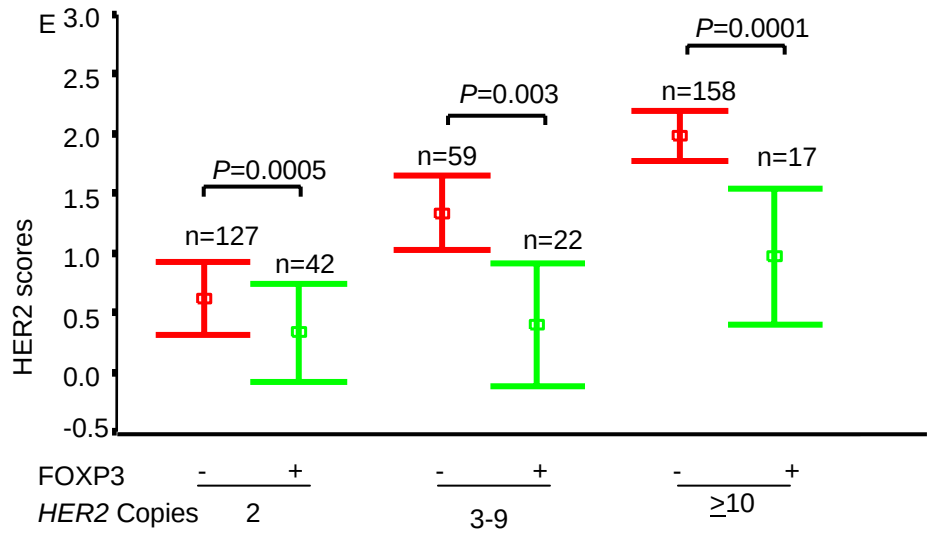
E
3.0
2.5
2.0
1.5
1.0
0.5
0.0
-0.5
HER2 scores
P=0.0005
P=0.003
P=0.0001
n=127
n=42
n=59
n=22
n=158
n=17
FOXP3
-
+
-
+
-
+
HER2 Copies
2
3-9
≥10

Fig. 6-2

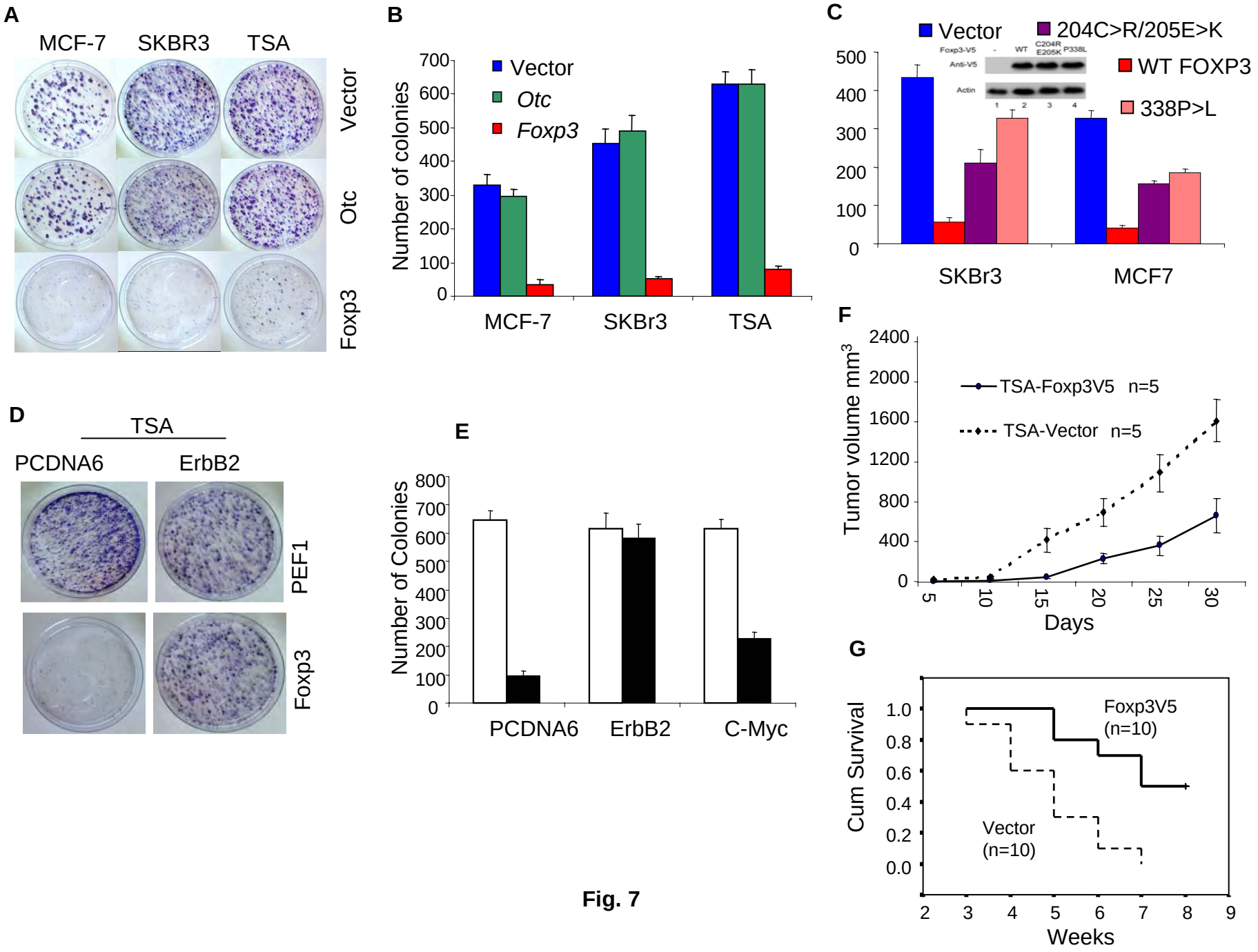
A
MCF-7
SKBR3
TSA
Vector
Otc
Foxp3
B
Number of colonies
Vector
Otc
Foxp3
MCF-7
SKBr3
TSA
C
Vector
204C>R/205E>K
WT FOXP3
338P>L
SKBr3
MCF7
D
TSA
PCDNA6
ErbB2
PEF1
Foxp3
E
Number of Colonies
PCDNA6
ErbB2
C-Myc
F
Tumor volume mm3
TSA-Foxp3V5 n=5
TSA-Vector n=5
Days
G
Cum Survival
Foxp3V5
(n=10)
Vector
(n=10)
Weeks

Fig. 7